Journal Pre-proof

Novel naphthylamide derivatives as dual-target antifungal inhibitors: Design, synthesis and biological evaluation

Yunfei An, Yue Dong, Min Liu, Jun Han, Liyu Zhao, Bin Sun

PII: S0223-5234(20)30963-6

DOI: https://doi.org/10.1016/j.ejmech.2020.112991

Reference: EJMECH 112991

To appear in: *European Journal of Medicinal Chemistry*

Received Date: 4 September 2020

Revised Date: 15 October 2020

Accepted Date: 31 October 2020

Please cite this article as: Y. An, Y. Dong, M. Liu, J. Han, L. Zhao, B. Sun, Novel naphthylamide derivatives as dual-target antifungal inhibitors: Design, synthesis and biological evaluation, *European Journal of Medicinal Chemistry*, https://doi.org/10.1016/j.ejmech.2020.112991.

Graphical Abstract

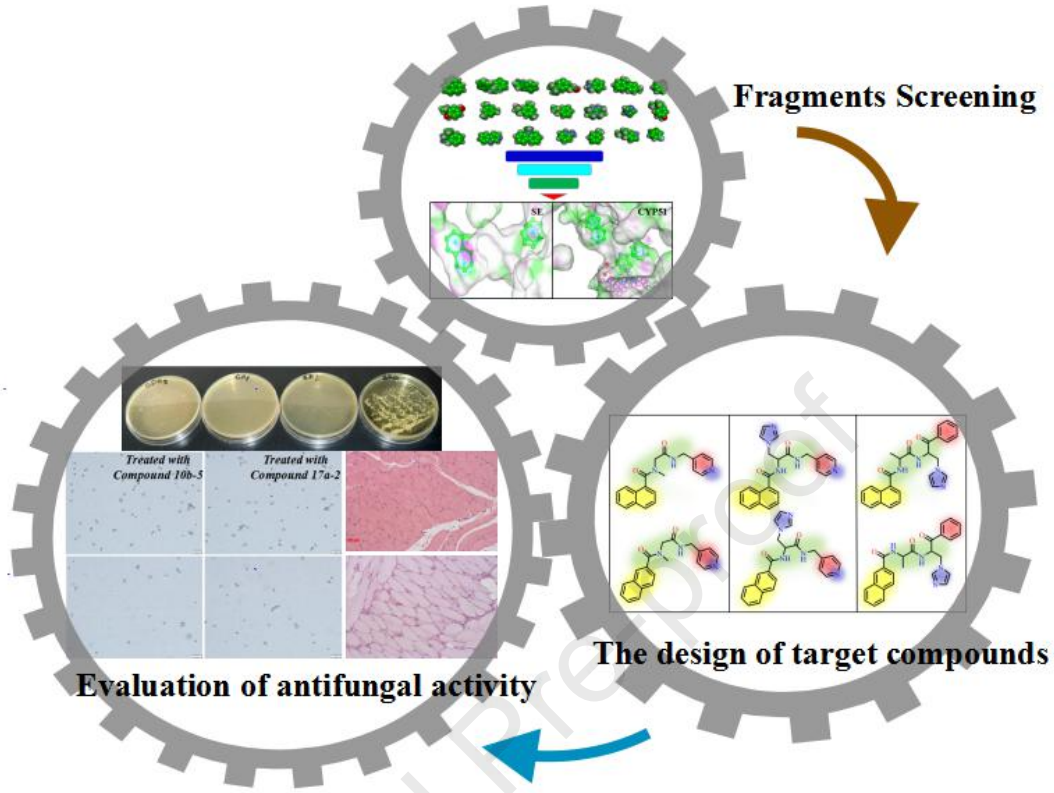

Novel naphthylamide derivatives as dual-target antifungal inhibitors: Design, synthesis and biological evaluation

Yunfei An [a, 1], Yue Dong [a, 1], Min Liu [a], Jun Han [a], Liyu Zhao [b], Bin Sun [a,*]

[a] *Institute of BioPharmaceutical Research, Liaocheng University, 1 Hunan Road, Liaocheng 252000, PR China*

[b] *Key Laboratory of Structure-Based Drug Design & Discovery of Ministry of Education, School of Pharmaceutical Engineering, Shenyang Pharmaceutical University, 103 Wenhua Road, Shenhe District, Shenyang 110016, PR China*

[1] *Both authors contributed equally to this study*

[*] *Corresponding anthor: Bin Sun, E-mail: sunbin19840104@163.com*

ABSTRACT:

Fungal infections have become a serious medical problem due to the high infection rate and the frequent emergence of drug resistance. Squalene epoxidase (SE) and 14α-demethylase (CYP51) are considered as the important antifungal targets, they can show the synergistic effect on antifungal therapy. In the study, a series of active fragments were screened through the method of De Novo Link, and these active fragments with the higher Ludi_Scores were selected, which can show the obvious binding ability with the dual targets (SE, CYP51). Subsequently, three series of target compounds with naphthyl amide scaffolds were constructed by connecting these core fragments, and their structures were synthesized. Most of compounds showed the antifungal activity in the treatment of pathogenic fungi. It was worth noting that compounds **10b-5** and **17a-2** with the excellent broad-spectrum antifungal properties also exhibited the obvious antifungal effects against drug-resistant fungi. Preliminary mechanism study has proved these target compounds can block the biosynthesis of ergosterol by inhibiting the activity of dual targets (SE, CYP51). Furthermore, target compounds **10-5** and **17a-2** with low toxicity side effects also demonstrated the excellent pharmacological effects in *vivo*. The molecular docking and ADMET prediction were performed, which can guide the optimization of subsequent lead compounds.

Key Words: Fungal infections; Dual-Target; Inhibitors; Organic synthesis; Antifungal activity

`

1. Introduction

Over the past two decades, the incidence of fungal infections has been increasing dramatically, especially the emergence of systemic fungal infection and fungal resistance, it has presented a serious threat to human health [1,2,3]. These infections occurrence has resulted from many factors, such as the widespread abuse of broad-spectrum antibiotics, immunosuppressants, radiotherapy and chemotherapy drugs in clinic, which seriously destroyed the normal physiological function in human body [4-7]. However, we have lacked of the effective treatment for these fungal diseases. This requires us to constantly develop new antifungal drugs to cope with the growing problems.

At present, the clinically available antifungal agents can be divided into two different classes based on their structure characteristics, including antibiotics (e.g., polyenes, echinocandins) and small molecular compounds (e.g., azoles, acrylamines and 5-fluorocytosine) [8-11]. Of those, acrylamines and azole antifungal agents as small molecular compounds are currently most widely used in first-line antifungal therapy (**Figure 1**), especially there has still a large number of azoles compounds reported constantly [12-15]. They can block the ergosterol biosynthesis by inhibiting separately the activity of squalene epoxidase (SE) and 14α-demethylase (CYP51) [16,17,18]. When the ergosterol content decreased, fungal cell permeability and osmotic pressure would change [19,20]. At the same time, some toxic endogenous intermediates (e.g., lanosterol and 14a-methyl-3-6-diol) also were accumulated rapidly in the fungal cells, which eventually lead to fungal death [21,22]. In addition, azoles (e.g., miconazole, fluconazole, albaconazole) and acrylamides (e.g., butenafine, terbinafine, naftifine) drugs can also be selected as the combination drugs to treat fungal infection, especially for the drug-resistant emergence of pathogenic fungi [23,24]. They exhibited the obvious synergistic effects and excellent antifungal activity in *vitro* [25]. However, several factors have limited their practical applications, such as uneven absorption, cytotoxicity, drug resistant and low bioavailability [26,27]. Therefore, there is still an urgent task to develop novel antifungal agents. Dual-target drugs or multi-target drugs can avoid these disadvantages through the simultaneous inhibition of signaling pathways [28,29]. Dual-target or multi-target drugs can regulate multiple links in the disease network system by combining more than two targets. The resulting synergy effect improve the efficacy of drugs and reduce the development of drug resistance. In addition, these inhibitors generally have weak affinity with biological targets, which can greatly reduce the occurrence of adverse drug reactions [30,31]. Based on this principle, we aimed to construct the novel dual-target antifungal inhibitors by analyzing the active sites of dual-target (SE, CYP51).

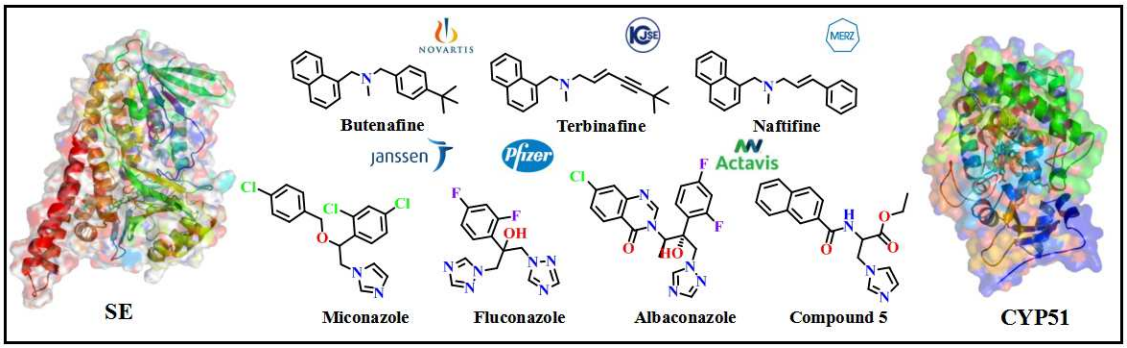

Figure. 1 Structure of target enzymes (SE, CYP51) and the representative acrylamines (SE inhibitors) and azole antifungal agents (CYP51 inhibitors).

In the study, we studied the structural characteristics of acrylamine and azole drugs, and constructed the different series of novel dual-target (SE, CYP51) antifungal inhibitors using the method of fragment-based drug discovery (FBDD). Subsequently, these target compounds were further synthesized, and their antifungal activity were evaluated in *vivo* and *vitro*. At the same time, the preliminary action mechanism was also explored and proved using cell-based and biochemical assays. This study will provide a new direction to design the novel dual-target antifungal inhibitors.

2. Results and discussion

2.1. Dual-target docking study based on active fragments

With the development of protein structure diffraction technology, the crystal structure of CYP51 has been resolved and studied [32]. At the same time, the homology model of SE has also been constructed in our previous study [33]. However, it is still a great challenge to discover the corresponding target inhibitors. This is because their binding conformation is difficult to be determined in the conventional molecular screening process. De novo drug design is a brand-new method of fragment-based drug discovery (FBDD) [34,35]. It can be used to more accurately determine the location, orientation and conformation of the core fragments in the different active sites.

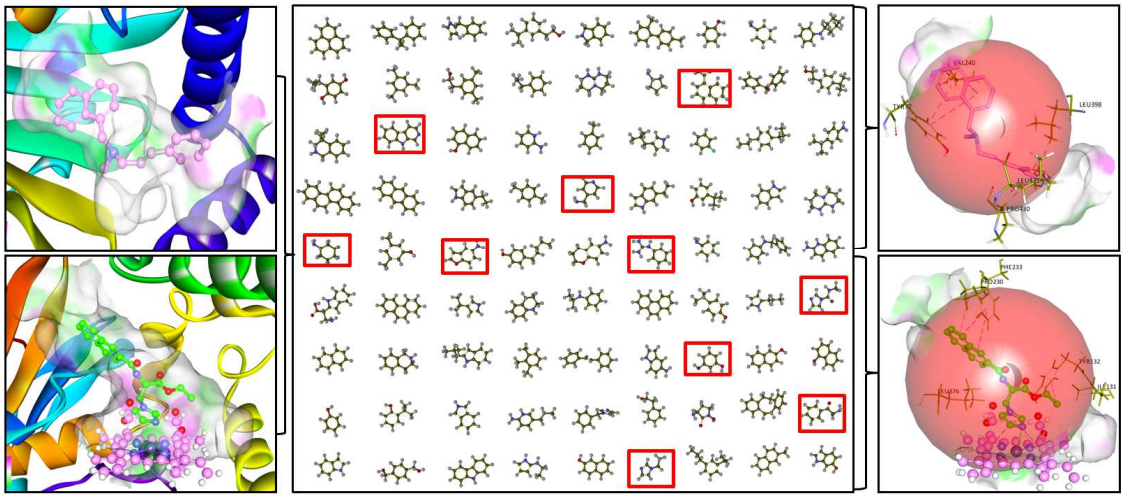

Figure. 2. The screening of active fragments based on the active sites of dual-target enzymes (SE, CYP51).

The drug-like fragment library was constructed, which contain a series of different kinds of organic fragments. De Novo Link, which can attach new fragments based on the existing active groups, was selected as a classical important fragment docking method, and the value of Ludi_Score can accurately reflect the binding ability of docking fragments in active site (**Figure 2**). In the study, these active fragments in library were docked into the active sites of dual-target (SE, CYP51). Some of organic fragments demonstrated the strong binding ability, they can simultaneously produce this strong interaction force with the key amino acid residues, which distributed in the different active sites. Ten preferred fragments with high value of Ludi_Score were selected and determined, which were summarized in **Table 1.**

Table 1. The scoring values for preferred docking fragments

Name	Fragment structure	Potential Energy	Ludi_Score	
			SE	CYP51
1. 1-naphthoic acid	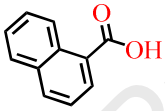	104.9261	331	348
2. 5-Amino-1-benzofuran	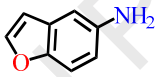	98.9786	279	316
3. Aminomethyl pyridine	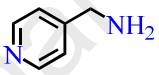	83.0628	308	324
4. 9*H*-pyrido[3,4-*b*] indole	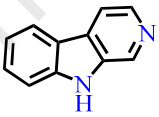	49.2029	287	301
5. 1-ethyl-1H-imidazole	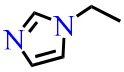	97.1579	301	298
6. N-methyl-1H-imidazole-1 -carboxamide	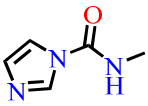	72.7368	284	296
7. 2-Aminoacetophenone	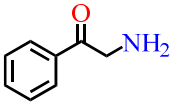	103.2519	314	291
8. N-phenylmethanetriamine		49.0356	252	280
9. Cyclohexaneamine	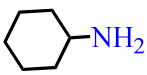	55.6181	279	264
10. Resorcinol	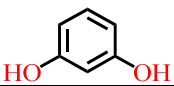	86.6885	249	237

Subsequently, we analyzed the structures of the inhibitors (SE inhibitor: naftifine; CYP51 inhibitor: compound **5**) [30,33] and their binding mode in their corresponding active sites. These screening fragments (**1**, **2**, **4**) were located in their upper region of active sites (SE, CYP51). Among them, the naphthyl fragment (**1**) with the highest value of Ludi_Score (SE: 331; CYP51: 348) can form the most stable interactions with the surrounding key amino acid residues, which were distributed in the active regions (A) (**Figure 3 A_1-A_3**). Moreover, it also is the main chain group of compound **5** (CYP51 inhibitor) and naftifine (SE inhibitor). Therefore, we discarded the active fragments (**2**, **4**), and selected to retain the naphthyl fragment as the main chain group to design the new target compound. In addition, we further analyzed the active site characteristics of the dual target, it can be seen that their hydrophobic feature groups were distributed in the all central region of active sites (SE, CYP51), which indicates that organic fragments should retain a certain of hydrophobic properties (**Figure 3 B_1-B_2**). Based on the above result, we found that these screening fragments **(3, 5, 7, 9)** with the proper scoring value can satisfy a certain degree of hydrophobic properties, they were distributed in the active regions (B, C), and produced the proper superposition phenomenon with ligand molecules in the active sites of dual-target (SE, CYP51). It is noteworthy that these nitrogen-containing fragments (**3, 5**) can also form the key coordination bonds interaction with heme in active site of CYP51 (**Figure 3 C_1-C_2**).

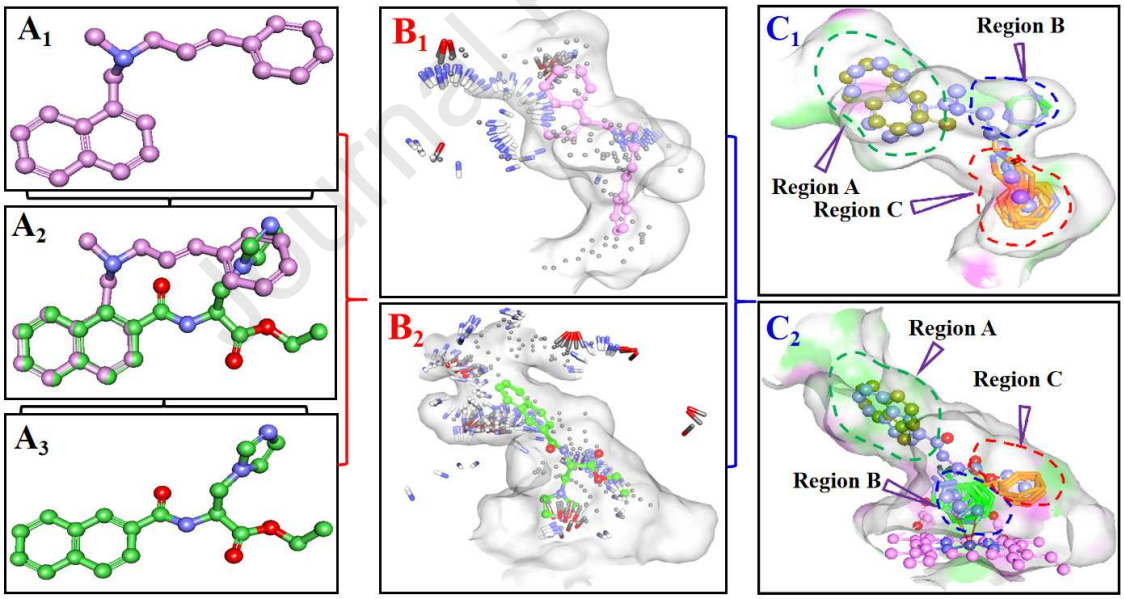

Figure. 3. (A_1-A_3) The superposition model based on the structure of terbinafine and compound 5. **(B_1-B_2)** The distribution of feature groups in SE and CYP51 active site. **(C_1-C_2)** The combination pattern of active fragments in the active regions of SE and CYP51.

2.2. The design of antifungal agents

On this basis, three series of dual-target target compounds with the common naphthyl fragment as main chain group were designed based on the different splicing methods of active fragments (**Figure 4**). At first, the pyridyl fragment (**3**) can replace the phenyl

group of naftifine and the azole group of compound **5**, and exert their corresponding biological functions in the different active sites. Therefore, the pyridyl fragment (**3**) was selected as the core groups of dual-target target compounds. This specific connection method was performed to construct the series **1** target compounds (**Figure 4 A_1**). In addition, the phenyl and cyclohexane fragments (**7**, **9**) were bound into the region A of SE and the region B of CYP51, the imidazole fragment (**5**) was docked in the region B of SE and the region A of CYP51. Finally, these fragment combinations were connected as a whole, and the series **2, 3** target compounds were produced though the different connecting methods (**Figure 4 A_2, A_3**).

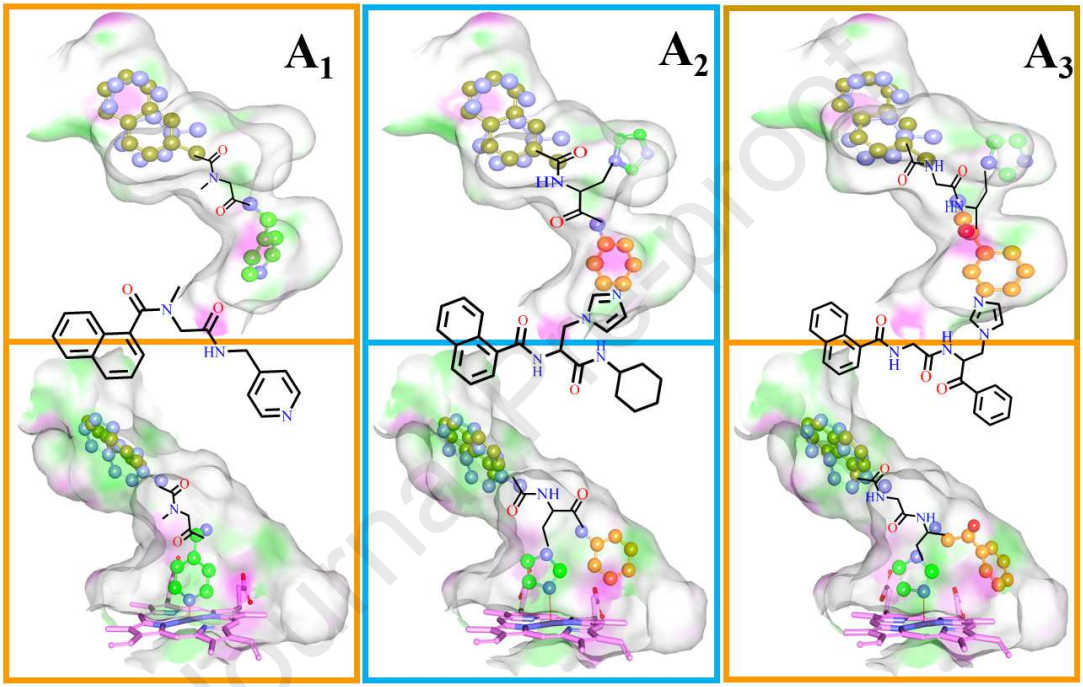

Figure 4. Design of naphthylamide derivatives as novel dual-target antifungal inhibitors using the method of FBDD.

In order to further verify the design rationality, these target compounds were docked into the active sites of SE and CYP51, respectively. They can be combined in the active sites of dual-target, and these core fragments were properly distributed in the key regions of the active sites (**Figure 5 A_1, A_2**). At the same time, these target compounds can also be superimposed with ligand molecules (SE inhibitor: naftifine; CYP51 inhibitor: compound **5**), and they show the higher matching degree. The result indicates that these target compounds can simultaneously satisfy the distribution characteristics of dual-target inhibitors (**Figure 5 B_1, B_2, B_3**). Based on the detailed analysis of dual-target (SE, CYP51) docking model and molecular superposition model, their structures were further modified and optimized as the leading compounds. We expected that these compounds may have the dual-target antifungal activity, and the subsequent biological activity evaluation has confirmed the design rationality.

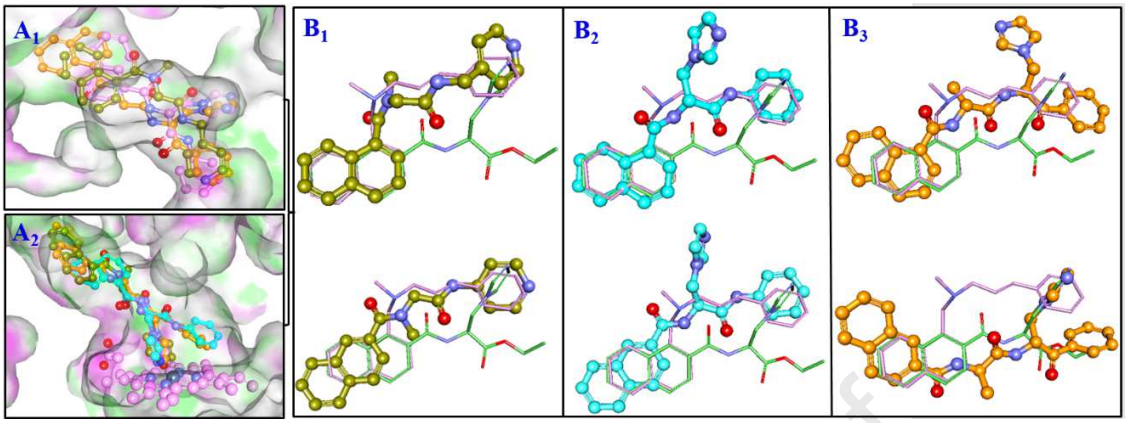

Figure 5. (A_1-A_2) Docking results of these representative target compounds with dual-target (SE, CYP51); **(B_1-B_3)** Molecular superposition model of target compounds with ligand molecular (naftifine, compound **5**).

2.3. Chemistry

The synthetic route of key intermediates **4a, b-1, 2, 3, 4** was illustrated in **Scheme 1**. The commercially available L-Glycine, Glycine, Alanine, Valine, Serine (**2-1, 2, 3, 4**) were selected as the starting material, and they were dissolved in ethanol, and refluxed with $SOCl_2$ for 5 h, the amino acid ethyl ester hydrochloride (**3-1, 2, 3, 4**) were obtained [36]. Next, the amino acid ester hydrochloride was separately treated with the 1-naphthoic acid (**1a**) and 2-naphthoic acid (**1b**) in the presence of condensing agent to give the key intermediates (**4a, b-1, 2, 3, 4**). Target compounds **7a-1, 2, 3, 4** and **7b-1, 2, 3, 4** were prepared according the procedures, which was shown in **Scheme 2**. The methyl group was introduced into the key intermediates (**4a, b-1**) through methylation reaction, and formed the intermediates products (**5a, b-1**). Next, they can be directly hydrolyzed to obtain the corresponding organic acids (**6a, b-1**). Finally, the target compounds **7a, b-1, 2, 3, 4** were synthesized via amination reaction.

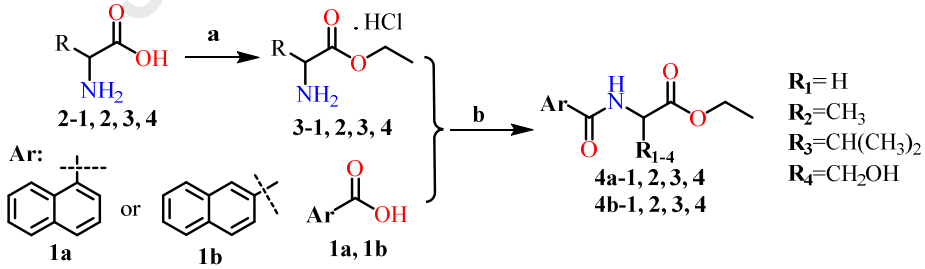

Scheme 1. Reagents and conditions: (a) Ethanol, $SOCl_2$, reflux, 2–5 h; (b) EDCI, HOBt, DIEA, 80 °C, 7h.

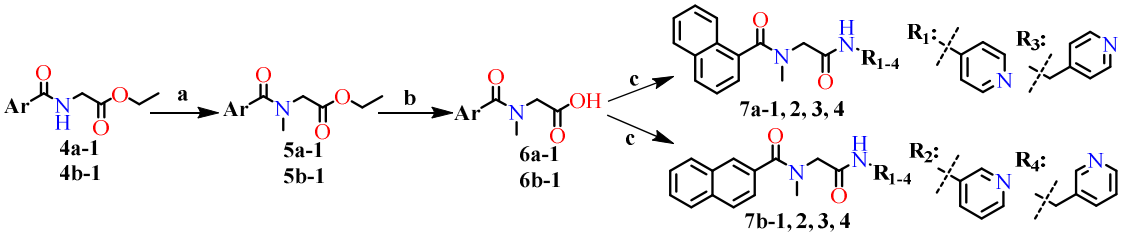

Scheme 2. Reagents and conditions: (a) CH_3I, K_2CO_3, THF, 60 °C, 5 h; (b) 2 N NaOH solution, MeOH, 60 °C, 2 h; (c) HATU, DIEA, DMF, amine (aminopyridine or aminomethyl pyridine), 80 °C, 7 h.

The synthetic route of the target compounds **10a, b-1, 2, 3, 4, 5** was illustrated in **Scheme 3**. First, the imidazole group was introduced into the key intermediates (**4a, b-4**) to afford the intermediate products **8a, b** [37]. Subsequently, they were further converted into the corresponding organic acids (**9a, b**) through hydrolysis reaction. Finally, the target compounds **10a, b-1, 2, 3, 4, 5** were synthesized from organic acids and aminomethylpyridine via amidation reaction.

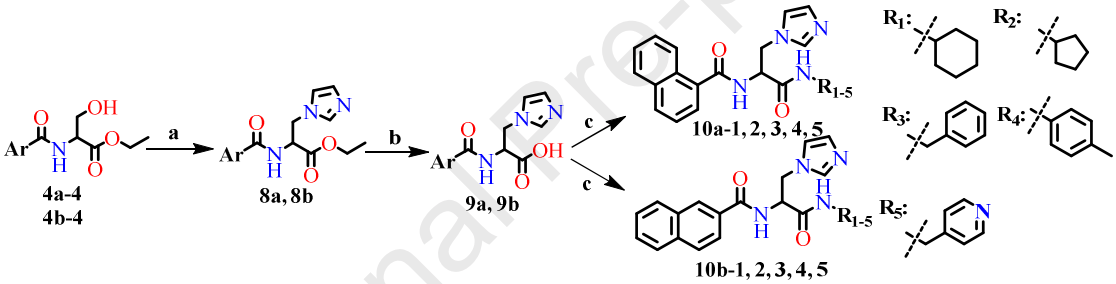

Scheme 3. Reagents and conditions: (a) CDI, imidazole, 70 °C, 3-5h; (b) 2 N NaOH solution, MeOH, 60 °C, 5 h; (c) HATU, DIEA, DMF, amine, 80 °C, 7 h.

The synthetic route of the target compounds **17a, b-1, 2, 3** and **18 a, b** was illustrated in **Scheme 4**. First, the key intermediates (**4a, b-1, 2, 3**) were hydrolyzed and converted into the corresponding organic acids (**11a, b-1, 2, 3**). Next, these organic acids (**6a, b-1; 11a, b-1, 2, 3)** were separately treated with the aminoacetophenone to obtain the key intermediates (**13a, b-1, 2, 3; 14a, b**). Subsequently, the treatment of intermediates was treated with formaldehyde and $NaHCO_3$ in $MeOH/H_2O$ to produce the hydroxyl compounds (**15a, b-1, 2, 3; 16a, b)** [38]. Finally, these compounds (**15a, b-1, 2, 3; 16a, b)** were further reacted with CDI and imidazole to obtain the target compounds (**17a, b-1, 2, 3; 18a, b**).

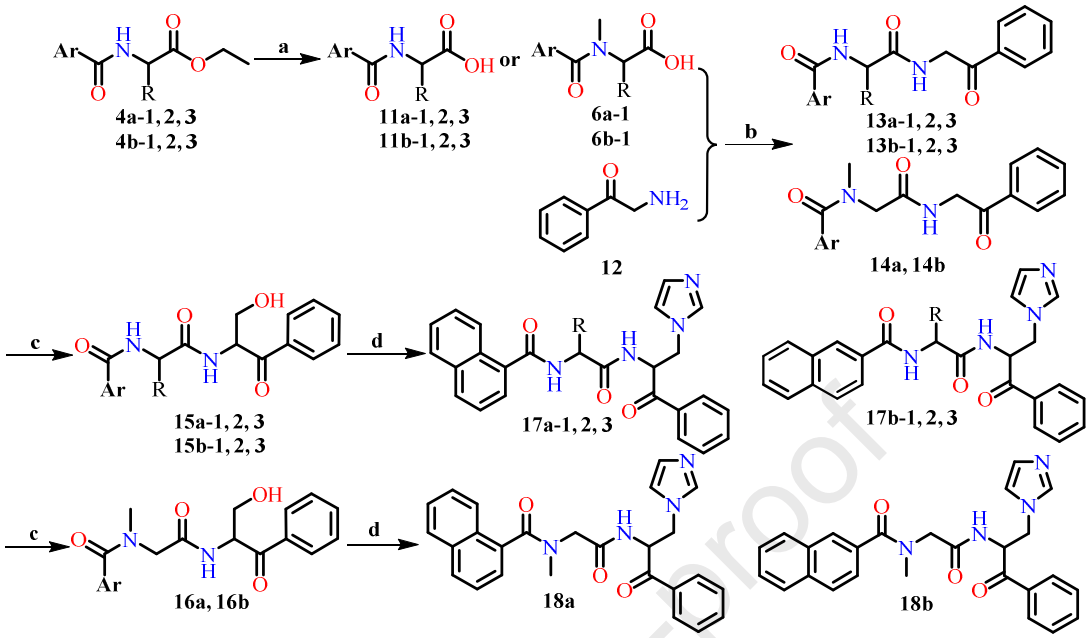

Scheme 4. Reagents and conditions: (a) 2N NaOH solution, MeOH, 60 °C, 2 h; (b) EDCI, HOBt, DIEA, 80 °C, 7h; (c) 37% CH_2O (aq), $NaHCO_3$, EtOH, 6 h; (d) Imidazole, CDI, CH_3CN, 70 °C, 5 h.

2.4. In vitro antifungal activity of target compounds

In the study, all target compounds were selected to evaluate their in *vitro* antifungal activity against pathogenic fungi through the protocols of the National Committee for Clinical Laboratory Standards (NCCLS) [39,40], and the tested strain contains four pathogenic *Candida* (***C. alb.***, *Candida albicans*; ***C. gla.***, *Candida glabrata*; ***C. kru.***, *Candida krusei*; ***C. tro.***, *Candida tropicalis*) and one Aspergillus (***A. fum.***, *Aspergillus fumigatus*). Naftifine and fluconazole (FCZ) were selected as the reference drugs.

The antifungal activities of target compounds were summarized in **Table 2**. It was observed that most of compounds exhibited the antifungal activity against ***C. alb.***, ***C. gla.***, ***C. kru.*** and ***C. tro.*** in *vitro*. These target compounds, which contain **7a-2, 7b-2, 7b-4, 10a-4, 10a-5, 10b-1, 10b-4, 10b-5, 17a-1, 17a-2, 17b-2, 18a** and **18b,** showed a certain of antifungal activity against *Candida* in the range of 0.125-0.5 μg/mL. Of these, these target compounds (**7b-2, 10b-4**, **10b-5**, **17a-1**, **17a-2** and **18b**) with the range of MIC_{50} value (0.125-0.25 μg/mL) against *C.alb*, *C.gla.* and *C.tro.*, which can show the similar potency with the control drugs (fluconazole: 0.25 μg/mL, naftifine: 0.25-0.5 μg/mL). In addition, the target compounds (**7b-2, 7b-4, 10b-4, 10b-5, 17a-2, 17b-2** and **18b**) also exhibited the obvious antifungal activities against *C.kru.* with 0.25 μg/mL. However, most of compounds have an unsatisfactory inhibitory effect on *A. fum.* It was noteworthy that compounds **7b-2, 10b-5** and **17a-2** shows the most potent activity against *A.fum.* with MIC_{50} values 4 μg/mL. Subsequently, we preliminarily analyzed the structure-activity relationship of target compounds. It should be mentioned that the different position of naphthyl fragment as main chain can retain a certain effect on antifungal activity. At the same time, the change of side chain fragments can increase the

antifungal activity and the antibacterial spectrum. It was worth noting that the pyridine group can also replace azole group to maintain the antifungal activity.

Table 2. *In vitro* antifungal activities of the target compounds (MIC_{50}, μg/mL).

Compd	R	MIC_{50}, μg/mL				
		C.alb.	***C.gla.***	***C.kru.***	***C.tro.***	***A.fum.***
7a-1	4-aminopyridine	0.5	0.5	0.5	1	8
7a-2	3-aminopyridine	0.25	0.25	0.5	0.25	>16
7a-3	4-pyridinemethaneamine	1	1	2	0.5	8
7a-4	3-pyridinylmethylamine	0.5	2	0.5	0.25	>16
7b-1	4-aminopyridine	0.25	0.5	1	0.25	8
7b-2	3-aminopyridine	0.125	0.25	0.25	0.125	4
7b-3	4-pyridinemethaneamine	0.25	2	0.5	1	8
7b-4	3-pyridinylmethylamine	0.5	0.5	0.25	0.25	>16
10a-1	cyclohexanamine	0.5	0.25	0.5	1	>16
10a-2	cyclopentanamine	0.5	2	0.5	0.5	>16
10a-3	phenylmethanamine	0.5	0.5	1	0.25	8
10a-4	4-methylaniline	0.25	0.25	0.5	0.5	>16
10a-5	4-pyridinemethaneamine	0.25	0.5	0.5	0.25	8
10b-1	cyclohexanamine	0.5	0.25	0.5	0.5	>16
10b-2	cyclopentanamine	0.25	0.25	1	0.5	8
10b-3	phenylmethanamine	0.5	1	1	0.5	>16
10b-4	4-methylaniline	0.125	0.25	0.25	0.25	8
10b-5	4-pyridinemethaneamine	0.25	0.125	0.25	0.25	4
17a-1	H	0.25	0.25	0.5	0.125	8
17a-2	methyl	0.125	0.25	0.25	0.125	4
17a-3	Isopropyl	0. 25	0.5	1	0.5	>16
17b-1	H	0.25	1	0.5	0.25	>16
17b-2	methyl	0.25	0.5	0.25	0.125	8
17b-3	Isopropyl	0.5	1	1	0.5	>16
18a	H	0.5	0.25	0.5	0.25	8
18b	H	0.125	0.25	0.25	0.25	8
Fluconazole	-	0.25	0.25	1	0.25	>16
Naftifine	-	0.5	0.25	2	0.5	8

Abbreviations: ***C. alb.***, *Candida albicans* (ATCC 10231); ***C. gla.***, *Candida glabrata* (ATCC 0001); ***C. kru.***, *Candida krusei* (ATCC 6258); ***C. tro.***, *Candida tropicalis* (ATCC 1369); ***A. fum.***, *Aspergillus fumigatus* (KM8001).

2.5. In vitro antifungal activity against fluconazole-resistant strains of Candida albicans

Currently, azole antifungal agents, especially fluconazole, have been widely applied in the clinical practice for many years, they have produced the excellent treatment effect.

However, the emergence of drug-resistant fungi has become more and more frequent, which has been an important medical problem for treating shallow and systemic fungal infection. Therefore, it's very important to further investigate the biological activity of target compounds against fluconazole-resistant strains. In the study, these fluconazole-resistant strain 17#, CaR, 632, 901 and 904 of *C.alb.* were selected as the test strains. Of there, strain 17# and strain CaR were isolated from AIDS patients. The result was shown in **Table 3.** The potent compounds **(7b-2, 10b-5, 17a-2)** and the reference drugs (fluconazole, naftifine) were selected to evaluate their antifungal activity. Fluconazole was inactive against the fluconazole-resistant strains with the MIC_{50} values > 16 μg/mL. Compounds **(7b-2, 10b-5, 17a-2)** and naftifine exhibited the moderate antifungal activities against strains 17# and CaR with MIC_{50} values in the range of 2-8 μg/mL. In addition, compounds **10b-5** and **17a-2** also displayed a certain of antifungal activity against strains 632 and 901 with MIC_{50} values in the range of 4-8 μg/mL. It's worth noting that compound **17a-2** showed the the best antifungal activity against fluconazole-resistant strains 17#, CaR and 901 with MIC_{50} values in the range of 2-4 μg/mL.

Table 3. *In vitro* antifungal activities of the target compounds (MIC_{50}, μg/mL).

Compd	**MIC_{50}, μg/mL**				
	Strain 17#	Strain CaR	Strain 632	Strain 901	Strain 904
7b-2	8	4	>16	>16	>16
10b-5	4	8	8	4	>16
17a-2	2	4	8	4	4
Naftifine	8	>16	8	>16	8
Fluconazole	>16	>16	>16	>16	>16

Abbreviations: strain 17#, **CaR**, **632, 901**, **904,** fluconazole-resistant strain of *Candida albicans*; **Strains 17#** and CaR were provided by Institute of Microbiology, Chinese Academy of Sciences. Strains 632, 901 and 904 were provided by the Second Military Medical University.

2.6. Density analysis of Candida albicans in different treatment groups

Observing the change of fungal cell density with different target compounds is an important index to evaluate the antifungal efficacy of target compounds. In the study, the untreated group and treated groups with positive control drugs (fluconazole, naftifine) and target compounds (**10b-5**, **17a-2**) were set, respectively. Their density was explored by polarizing microscopy in the particular concentrations (10 nm/mL).

In the untreated groups, *C. alb.* (ATCC SC5314) exhibited the significant proliferation ability, the density of fungal cells increased rapidly with the prolong of treatment time, and a large number of cell germination and spores were observed in nutrient solution **(Figure. 6 $A_{1,2}$)**. In the treated groups with positive control drugs and target compounds, the tendency of cell proliferation was obviously inhibited, and cell density has gradually decreased with the prolong of treatment time. The proportion of *Candida* cells in the division phase was significantly lower than the untreated group, and some cells even have the fracture phenomenon **(Figure. 6 $B_{1,2}$-$E_{1,2}$)**. These results indicated that the target

compounds (**10b-5**, **17a-2**) show the same antifungal effect with the positive control drugs (fluconazole, naftifine), they can significantly affect the changes of fungal cell density by inhibiting the fungal cells proliferation.

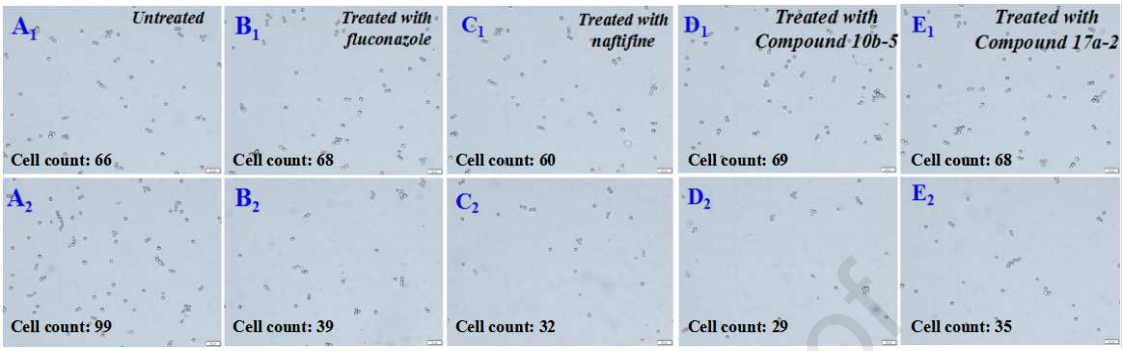

Figure 6. The density changes of fungal cell in different treatment groups. (**A_1-A_2**: Untreated; **B_1-B_2**: Fluconazole; **C_1-C_2**: Naftifine; **D_1-D_2**: Compound **10b-5**; **E_1-E_2**: Compound **17a-2**).

In order to further evaluate the antifungal efficacy of target compounds (**10b-5**, **17a-2**). The survival and mortality rates of *C. alb.* in different treatment groups were studied. The results showed that the survival rate of fungal cells was as high as 97% in untreated group, and cell size exhibits the state of uniform distribution (**Figure 7**). In the treated groups with target compounds (**10b-5**, **17a-2**), their survival rates of fungal cells fall to the 16% and 11%, respectively. Moreover, the sizes of living fungal cells also decreased to 7.53 μm and 7.51 μm from the 8.29 μm. The result further confirmed that compounds **10b-5** and **17a-2** can significantly affect the physiological functions of fungal cell, they not only can effectively inhibit the fungal cell proliferation, but also can kill the existing fungal cells.

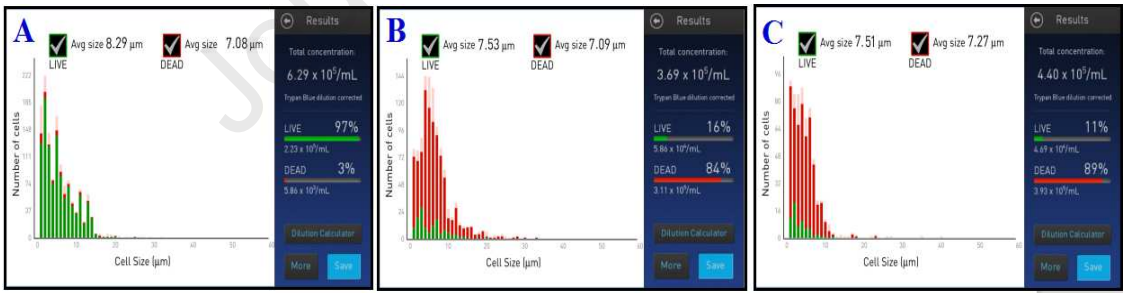

Figure 7. The survival and mortality rate of *C. alb.* cells in different treatment groups (**A**: untreated; **B**: compound **10b-5**; **C**: and compound **17a-2**).

2.7. Morphological analysis of Candida albicans in the treatment groups with target compounds 17a-2

In order to further understand the effect of preferred compound **17a-2** on the cell morphology, the morphological changes of the *Candida* cells were observed using transmission electron microscopy (TEM) [41,42]. At the early stage, the structure of *C. alb.*, cells mostly exists in the shape of ellipse. Cytoplasm was uniformly distributed in the inner region of the fungal cells. The fungal cell membrane and wall were located at

the edge of cells. Their boundary can be clearly distinguished, and show the smooth and transparent characteristics (**Figure 8 A_1-A_2**). When the fungal cells were treated with compound **17a-2** for 72h, the clear boundary between the colony cell population began to disappear, and the smooth surfaces changed into the irregular structure. At the same time, some specific phenomena occurred in the cytoplasmic regions, such as edema cavitation, disordered ridge arrangement, and exfoliation of rough endoplasmic reticulum particles (**Figure 8 B_1-B_2**). With the further prolongation of treated time (144h), the fungal cells have completely cracked, only residual fungal cell wall and membrane structure were left (**Figure 8 C_1-C_2**). The preliminary result suggests that the target compound **17a-2** can destroy the structure of cell membrane and affect the osmotic pressure of fungal cell. It can eventually lead to the rupture and death of fungal cells.

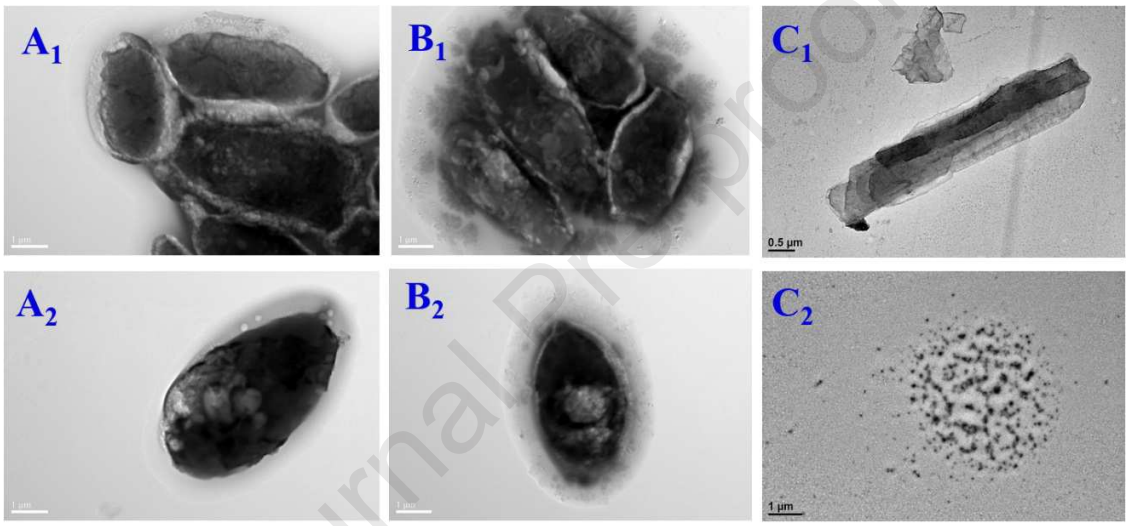

Figure 8. The morphological structure changes of *C. alb.* cells treated with target compound **17a-2** in the different time periods. (**A_1-A_2**: 0 h; **B_1-B_2**: 72h; **C_1-C_2**: 144h).

2.8. Molecular mechanism and enzyme activity of target compounds

In order to further study the antifungal mechanism of target compounds (**10b-5**, **17a-2**), the sterol composition change of *C. alb.* SC5314 cells in different treated groups were analyzed. The untreated group and positive control drugs (fluconazole, naftifine)-treated group were set as reference. The assay has been successfully used in studying the action mechanism of antifungal agents on the sterol biosynthesis pathways [35, 42]. The sterol profifile results were summarized in **Table 4**.

Table 4. Analysis of sterol composition in *C.alb.* by LC-MS.[a]

Compd.	**Concentration (μg/mL)**	% of total sterols (*C. alb.*)				
		Ergosterol	**Squalene**	**Lanosterol**	**Eburicol**	**Unknown sterol**
10b-5[b]	0.125	68.4	9.2	3.8	13.6	5.0
	0.5	35.6	14.5	7.2	37.9	4.8
	4	13.2	20.5	10.9	49.3	6.1
17a-2	0.125	66.4	7.9	2.8	17.5	5.4

	0.5	29.9	21.6	8.7	34.0	5.8
	4	10.8	27.9	12.5	42.6	6.2
Naftifine[c]	0.125	73.5	16.8	3.7	1.9	4.1
	0.5	40.8	39.2	9.4	5.7	4.9
	4	15.9	56.8	12.5	9.7	5.1
Fluconazole	0.125	78.5	-	5.1	12.8	3.6
	0.5	43.9	-	8.9	42.5	4.7
	4	12.7	1.3	16.3	64.5	5.2
Control[d]	-	95.1	-	-	1.4	3.5

[a] Abbreviations: *C.alb.*, *Candida albicans* (ATCC SC5314).

[b] Treated with target compounds **10b-5, 17a-2**.

[c] Treated with naftifine.

[d] Control (no drug).

In the untreated control, the content of ergosterol in the fungal cell membrane contained 95.1% of the sterol fraction, while squalene and lanosterol was not observed, and other unknown sterols contained only 3.5%. When *C. alb.* was treated with fluconazole at 0.125-4 μg/mL for 48 h, the content of ergosterol in the cell membrane decreased to 12.7% from 95.1%, the content of eburicol increased sharply to 56.8%, while squalene and lanosterol contents didn't increase significantly. These changes of this components are due to the competitive inhibition activity of target enzyme CYP51, which are consistent with previously published studies. In the treated group with naftifine, the content of ergosterol reduced to 15.9% from 95.1%, and the contents of squalene, lanosterol and eburicol were accumulated. In particular, the content of squalene increased sharply to 56.8%. These changes were caused by the competitive inhibition of CASE in *C. alb*. The ergosterol content was significantly reduced to 13.2% and 10.8%, respectively. Interestingly, the treatment with compounds **10b-5** and **17a-2** also resulted in the noticeable accumulation of squalene (20.5%, 27.9%) and eburicol (49.3%, 42.6%), These results suggested that these novel compounds can caused the potent disruption of ergosterol biosynthesis by inhibiting the double-target (SE, CYP51) activity in *C. alb.*, which was similar with the accepted mechanism of fluconazole and naftifine. Subsequently, the dual-target (SE, CYP51) enzymatic activity of compounds **10b-5** and **17a-2** was tested (**Table 5**). Compared with naftifine (SE, IC_{50} = 0.284 μM) and fluconazole (CYP51, IC_{50} = 0.116 μM), they displayed a certain degree of dual-target enzymatic activity with IC_{50} values ranging from 0.537-1.153 μM, the study further proved their dual-target inhibitory activity.

Table 5. The dual-target (SE, CYP51) enzymatic activity of compounds 10b-5 and 17a-2

Compd	IC_{50} (μM)	
	SE	CYP51
10b-5	0.685	1.153
17a-2	0.961	0.537
Naftifine	0.284	-

Fluconazole	-	0.116

[a] Used as positive control.

2.9. In vitro human plasma stability assay

The stability of the target compound in human plasma is an important indicator to maintain the medicinal property [42]. Based on their antifungal activities in *vitro*. Compounds **10b-5** and **17a-2** were further selected to evaluate its stability in human plasma. In the study, these target compounds **10b-5** and **17a-2** were incubated in human plasma for 60 min and 120 min, respectively. Their result was shown in **Table 6**, these target compounds exhibited the excellent metabolic stability at same times (120 min: remaining 91.6% and 92.1%, respectively), which indicate that these compounds can maintain their medicinal efficacy in *vivo* for a long time.

Table 6. In *vitro* human plasma stability of compounds 10b-5 and 17a-2.

Compd.	Stability in Human Blood Plasma	
	% Remaining at 60 min	% Remaining at 120 min
10b-5	94.5	91.6
17a-2	96.3	92.1

2.10. In vivo study of toxicity and therapeutic efficacy

The potential toxicity and therapeutic effect of new target compounds in *vivo* is an important index during the process of new drug development. The pharmacodynamic properties of the preferred compound **10b-5** and **17a-2** were further evaluated in mice [42].

In this study, we constructed the fungal infection mouse models by subcutaneous injection, and the body weights of mouse in these different treatment groups were monitored, and their body weights did not display the significant differences during the whole treatment period. *H&E* (hematoxylin–eosin staining) was performed to observe the morphology of tissue after in the different treated groups, which was shown in **Figure 9**.

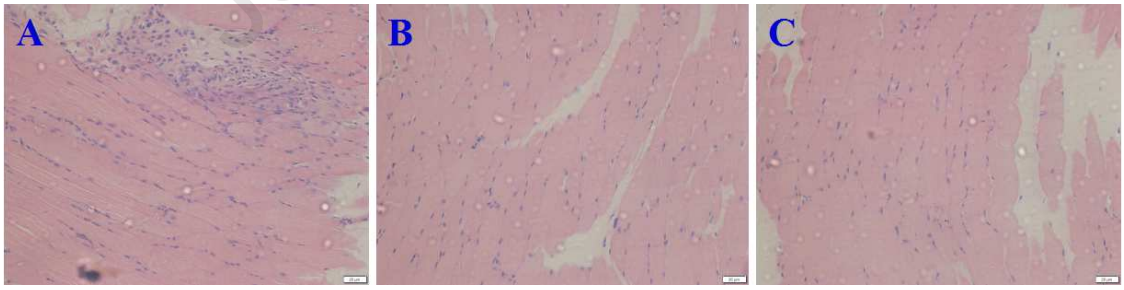

Figure 9. The morphological change of fungal infections tissues in different treatment groups (**A**: Saline; **B**: Compound **10b-5**; **C**: Compound **17a-2**).

In the treated group with saline, the arrangement of endothelial tissue cells begins to display the irregular distribution characteristics, the space of some endothelial cells increases significantly, and their configuration also undergoes a certain change. At the same time, a large number of nuclear gathers in the infected region was observed, which indicates that the pathogenic fungal infection has appeared, and the region has produced the corresponding immune response. In the treated groups with target compounds **10b-5**

and **17a-2**, we found that these tissue cells reappeared the uniform distribution characteristics and the complete state in the fungal infection region. It is worth noting that the aggregation of cell nuclear in the infected region has also disappeared, which suggested that these target compounds can significantly treat the endogenous fungal infection, and the infected tissues have gradually returned to normal state. These *H&E* results further demonstrated the synergistic therapeutic effect of the compounds.

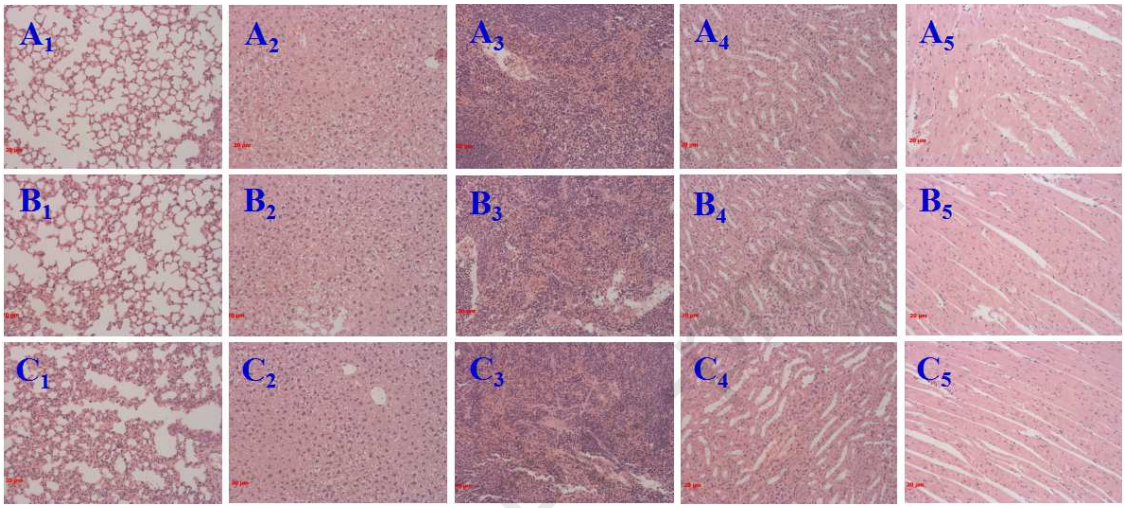

Figure 10. The histological images of *H/E* staining (lung, liver, spleen, kidney and heart) from the different treatment groups. (**A_{1-5}: Saline**; **B_{1-5}:** Compound **10b-5**; **C_{1-5}:** Compound **17a-2**).

Subsequently, the in vivo safety of the compounds was further evaluated. Their main organs (heart, liver, spleen, kidney, and lung) were separated and collected in the different treatment groups. The structures of the visceral tissue cells in these different treatment groups were similar, and they didn't show the obvious morphological changes or cell damage **Figure 10**. Moreover, the blood urea nitrogen (BUN), aspartate aminotransferase (AST) and the alanine aminotransferase (ALT) are important indexes that can directly reflect the function of kidney and liver. We can see that the AST, ALT and BUN levels didn't show the significant difference ($p>0.05$) in the different treatment groups, which indicated the compounds **10b-5** and **17a-2** did not have the obvious hepatic and renal toxicity (**Table 7**). In summary, the target compounds have the antifungal activity *in vivo*, and they can significantly inhibit the proliferation of fungi in mice with low toxicity.

Table 7. The analysis of plasma biochemical levels with different treatment groups

Group	AST(IU/L)	ALT(IU/L)	BUN (mmol/L)
Saline	104.7±5.2	105±8.3	6.8±0.4
Compound 10b-5	108.6±6.3	102±12.6	7.3±0.9
Compound 17a-2	112.3±5.9	106±7.4	6.4±0.7

2.11. Molecular docking

In order to better understand the binding mode of target compound **17a-2**, it was docked into the dual-targets enzymes (SE and CYP51) of *C. alb.*, using the CDOCKER program [43,44], the SE homology model and CYP51 (PDB: 5TZ1) served as the

docking templates to generate the binding mode. Images depicting the proposed binding modes were generated using PyMOL, and the results were shown in **Table 8** and **Figure 11**.

Table 8. Molecular docking results of target compound **17a-2** with dual-target (SE, CYP51)

Compd	-CDOCKER ENERGY	-CDOCKER INTERACTION ENERGY	Absolute Energy	Target Enzyme
17a-2	24.53	42.85	57.44	SE
17a-2	21.15	39.92	49.51	CYP51
Naftifine	34.65	47.72	60.67	SE
Fluconazole	27.72	44.76	65.94	CYP51

In the SE docking model, the binding energies of target compound (**17a-2**) (CDOCKER ENERGY: −24.53 kcal/mol; CDOCKER INTERACTION ENERGY: −42.85 kcal/mol) were lower than naftifine (CDOCKER ENERGY: −21.15 kcal/mol; CDOCKER INTERACTION ENERGY: −39.92 kcal/mol), which indicated the target compounds can form the more stable interactions than positive control naftifine. It can be seen that the active site of SE exhibited the long column shape, compound **17a-2** was properly docked into the active site, and its docking conformation were displayed in **Figure 11 A_1-A_3**. The naphthyl group of compounds **17a-2** can bind in the upper region of the active site, and form π-alkylation with the key amino acid residues (Tyr 77, Arg 134, Leu 249 and Tyr 251). In addition, the phenyl and imidazole groups were located in the bottom region, they can produce the hydrophobic bond interaction with Leu 398, Cys 416, Val 427 and Pro 430, respectively. At the same time, the compound **17a-2** also can properly docked into the active chamber of the CYP51 (**Figure 11 B_1-B_3**). The CDOCKER ENERGY and CDOCKER INTERACTION ENERGY values were predicted as −24.65 and −45.38 kcal/mol, respectively, which is close to the docking value of fluconazole (CDOCKER ENERGY: −21.15 kcal/mol; CDOCKER INTERACTION ENERGY: −39.92 kcal/mol). The naphthyl group was surrounded with the key hydrophobic residues (Pro 230, Phe 235, Leu376, His377, Tyr 505, and Ser 507), the interaction of π-alkylation with Pro 230 and Leu 376 was produced. It is worth noting that the imidazole group plays an important role, which occupied the bottom region of the active site. It can form the key coordination bonds with Fe^{3+} of heme (The coordinate bond length is 2.707 Å). Additionally, the phenyl group can form the π-π interaction with Phe 126. In summary, the docking result have confirmed that the target compounds can match well in the binding cavity of dual-target (SE, CYP51), and t form the stable combination mode.

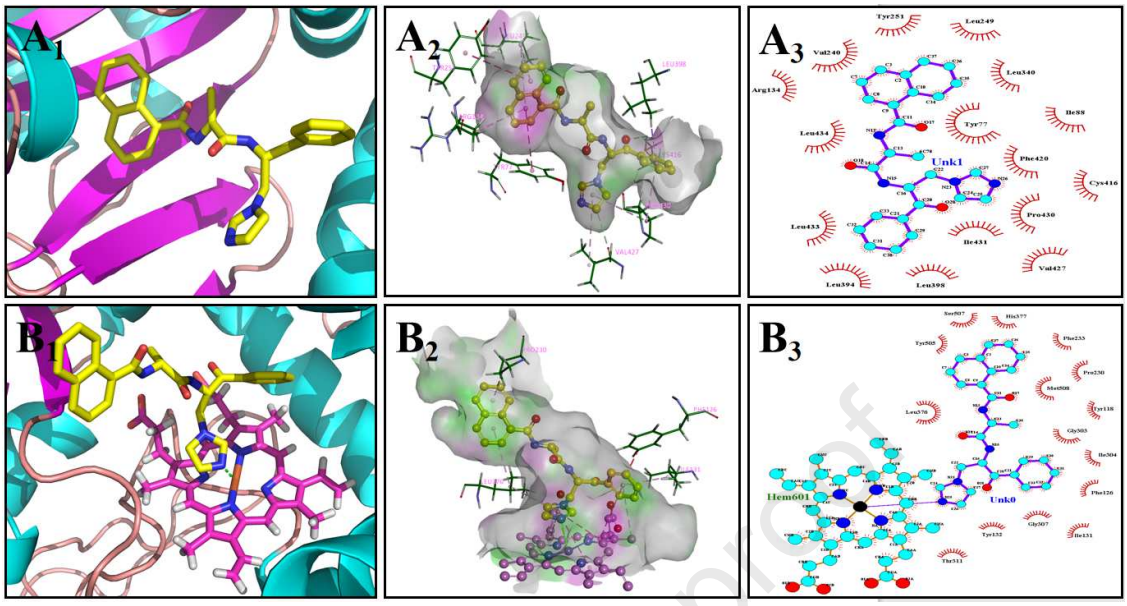

Figure. 11. Docking models of representative compound **17a-2** with dual-target (SE, CYP51). (**A_1**) The binding mode of the preferred compounds **17a-2** with CASE. (**A_2**) The interaction mode of compound **17a-2** in the active site of SE. (**A_3**) The interaction between the compound **17a-2** and SE on the 2D diagram. (**B_1**) The docking results of the preferred compounds **17a-2** with CYP51. (**B_2**) The interaction mode of compound **17a-2** in the active site of CYP51. (**B_3**) The interaction mode of compound **17a-2** in the active site of CYP51.

2.12. Theoretical evaluation of ADME/T properties

The properties of ADMET can reflect the process of the body's absorption, distribution, metabolism, and excretion of foreign chemicals. Therefore, the evaluation of ADMET properties is an important condition to ensure the drug-ability of the target compounds [45]. In the study, the ADME/T properties of target compounds were predicted, which was shown in **Figure 12.**

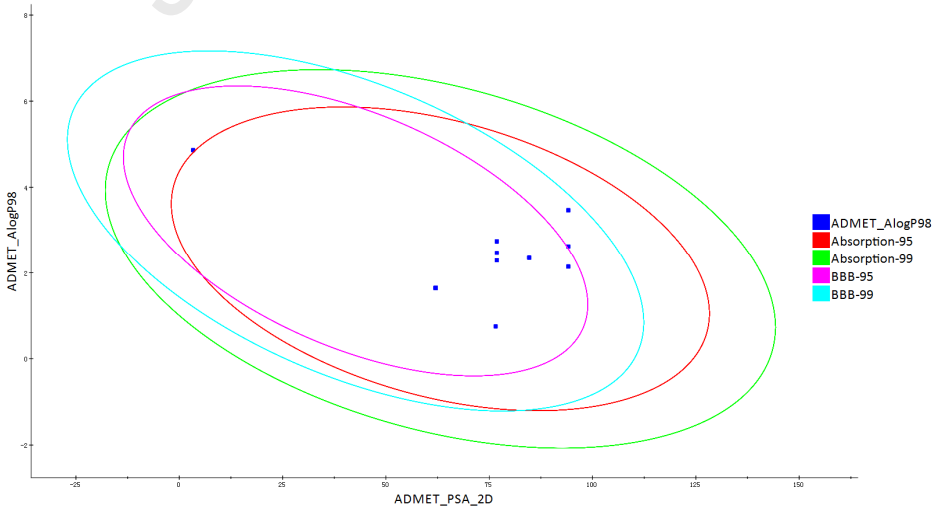

Figure 12. The evaluation plot of Alog P and PSA for the all target compounds. The 95% and 99% confidence limit ellipses that correspond to the intestinal absorption and BBB (blood-brain barrier) models. Abbreviations: ADME/T, absorption, distribution, metabolism, excretion and toxicity; A log P, the logarithm of the partition cofficient between octanol and water; PSA, polar surface area; 2D, two-dimensional.

The analogous 95% and 99% confidence ellipses for the blood-brain barrier (BBB) penetration and human intestinal absorption (HIA) was represented in the biplot **Figure 12**. All the target compounds and the control drug (fluconazole) were positioned in the confidence regions for HIA, which indicate these compounds have appropriate HIA properties. At the same time, most of compounds also have a certain permeability of blood-brain barrier, it reflects that these compounds have a certain therapeutic effect on fungal infection of nervous system.

Table 9. The ADME/T prediction of target compounds compared with naftifine and fluconazole.

ADME/T parameters	Series 1 compounds	Series 2 compounds	Series 3 compounds	Naftifine	Fluconazole
A log *P*98 [a]	1.638~1.645	2.139~2.741	2.139~3.466	4.863	0.750
PSA[b]	62.025	76.831	84.674, 94.132	3.352	76.556
Aqueous solubility	3	2, 3	2, 3	2	4
HIA[d]	0	0	0	1	0
PPB [e]	Highly bound	Highly bound	Highly bound	Highly bound	Highly bound
BBB penetration [f]	3	3	3	0	3
CYP450 2D6 binding [g]	0	0	0	0	1
Hepatotoxicity	Non-Toxic	Non-Toxic	Non-Toxic	Non-Toxic	Toxic
DTP [h]	Toxic, Non-Toxic	Toxic	Toxic	Toxic	Toxic
FDA[i] rodent carcinogenicity	Non-carcinogen	Non-carcinogen	Non-carcinogen	Non-carcinogen	Non-carcinogen
Ames mutagenicity	Non-mutagen	Non-mutagen	Non-mutagen	Non-mutagen	Non-mutagen
Skin sensitization	Non-irritant	Non-Irritant, Irritant	Non-Irritant, Irritant	Irritant	Irritant
Skin irritating	Non-irritant	Non-irritant	Non-irritant	Mild-irritant	Non-irritant

a. A log P98 (atom-based log *P*) (□-2.0 or □7.0: very low absorption). **b.** PSA (polar surface area) (>150: very low absorption). **c.** Level of aqueous solubility predicted: 0 (extremely low), 1 (very low, but possible), 2 (low), 3 (good), 4 (optimal), 5 (too soluble), 6 (warning: molecules with one or more unknown A log *P* calculations). **d.** HIA (human intestinal absorption), level of human intestinal absorption prediction: 0 (good), 1 (moderate), 2 (poor), 3 (very poor). **e.** PPB, plasma protein binding. **f.** BBB (blood brain barrier), level blood brain barrier penetration prediction: 0 (very high penetrate), 1 (high), 2 (medium), 3 (low), 4 (undefined). **g.** Prediction cytochrome P4502D6 enzyme inhibition (0: non-inhibitor; 1: inhibitor). **h.** DTP, development toxicity potential. **i.** FDA, food and drug administration.

These detailed values of ADME/T properties were summarized **Table 9.** The A logP and PSA of target compounds are the important properties of drug bioavailability. We can

see that the target compounds with PSA < 140, -2.0 < A logP < 7.0 have high oral bioavailability, these compounds have proper absorption or permeation, and they can be effectively absorbed in human intestine and highly bound with plasma protein. At the same time, those target compounds can also remain the Non-Hepatotoxicity, Low inhibitory activity on CYP450 2D6, which indicated that the target compound can maintain structural stability during the phase of metabolism. For toxicity risk, these compounds are non-carcinogenic, non-mutagenic and non-irritating. Although some of compounds demonstrate a certain degree of DTP and Skin sensitization, we believe that the further structural modifications can reduce the compounds' toxicity profiles.

3. Conclusions

At present, the phenomenon of invasive fungal infection and drug-resistant fungi is more and more frequent in clinical practice, which seriously threatens people's health. The design of dual-target (SE, CYP51) antifungal inhibitors was considered as an effective coping strategy. In the study, the corresponding fragment library was constructed by extracting the active groups of common antifungal inhibitors, and they were docked into the active sites of dual-target though the method of De Novo Link. These core groups with the higher MCSS_Score values were selected to design the fragment-based novel antifungal inhibitor. Subsequently, three series of target compounds were constructed and synthesized, their corresponding antifungal activity was evaluated. The most of target compounds exhibit the moderate or excellent antifungal activity. Among these, compounds **10b-5** and **17a-2** not only displayed the most remarkable in *vitro* activity against *Candida spp*. and *A. fum.*, but also had the obvious inhibitory effect on fluconazole-resistant *C.alb*. strains. In order to further understand the action mechanism of target compounds, the analysis of sterol composition and the study of dual-target enzyme inhibition were performed. The target compounds can block the biosynthesis of ergosterol and destroy the structure of fungal cell membranes by inhibiting the activity of dual-target (SE, CYP51). Notably, the compounds **10b-5** and **17a-2** with low toxicity and the excellent blood plasma stability also exhibited the obvious antifungal activity in *vivo*. At the same time, the target compounds can match well with the dual-target (SE, CYP51) binding cavity. In summary, these results demonstrate that these target compounds have the potential to be developed as the novel antifungal inhibitor.

4. Experimental section

4.1. General methods for chemistry

All reagents used in the experiment were procured from Energy Chemical, Aladdin, Bide and Sinopharm Company (except special instruction) without additional purification, and the solvents were purifified according to the standard procedures. The reactions were monitored by thin layer chromatography (TLC). and the analysis was performed on Silica Gel 60 F254 plates (Jiangyou, Yantai), which was used to monitor the reaction process. The silicagel (200-300 mesh) from Qingdao Ocean Chemicals (Qingdao, Shandong, China) was used for column chromatography. The melting points of all compounds were

determined and corrected with a Büchi Melting Point B-540 apparatus (Büchi Labortechnik, Flawil, Switzerland). The liquid chromatograph mass spectrometer (LC-MS) were determined in ESI mode on a Shimadzu 8040 LC-MS (Shimadzu, Japan). Nuclear magnetic resonance (^{1}H-NMR and ^{13}C-NMR) spectra were recorded on a Bruker 500 MHz NMR spectrometer with TMS as an internal standard. The coupling constants (J) are reported in Hertz, and the peak multiplicities were expressed as follows: s, singlet; d, doublet; t, triplet; q, quartet; dd, doublet of doublet; dt, doublet of triplet; td, triplet of doublet; ddd, doublet of doublet of doublet; m, multiplet; br, broad peak.

4.2. General procedure for the synthesis of amino acid ethyl ester hydrochloride (3-1, 2, 3, 4)

Thionyl chloride (3.0 equiv) was slowly dripped into the ethanol solution. Then, L-amino acids (Glycine, Alanine, Valine, Serine) (1.0 equiv) were dissolved in the mixed solution, respectively. The mixed solution was heated to reflux for 3-6 h. When the reaction liquid becomes transparent, the reaction mixtures were concentrated under reduced pressure to give the white solid **(3-1, 2, 3** and **4)**.

4.3. General procedure for the synthesis of key intermediate compounds (4a-1, 2, 3, 4; 4b-1, 2, 3, 4)

The appropriate 1-naphthoic acid and 2-naphthoic acid (1 equiv) and HATU (1.2 equiv) were added into anhydrous DMF, respectively. The mixture was stirred at room temperature for 2 h. Then, amino acid ethyl ester hydrochloride (**3-1, 2, 3, 4**;1.0 equiv) and DIEA (3.0 equiv) were added, the mixed solution was heated at 80 °C for 6 h. The reaction process was monitored by TLC analysis. After the completion of reaction, the reaction mixture was poured into ice water, and extracted with ethyl acetate, the organic phase was dried though Na_2SO_4 overnight. Finally, the desired intermediate compounds **(4a-1, 2, 3, 4; 4b-1, 2, 3, 4)** were obtained under vacuum distillation.

4.4. General procedure for the synthesis of compounds (5a-1; 5b-1)

The intermediate compounds (**4a-1** or **4b-1**; 1.0 equiv), K_2CO_3 (3 equiv) and CH_3I (2 equiv) were dissolved in tetrahydrofuran solution. Then, the mixed solution was stirred in the conditions of room temperature for 5 h. The reaction process was monitored by TLC analysis. After the completion of reaction, the mixture was poured into ice water, and extracted with ethyl acetate, the organic phase was dried by Na_2SO_4 overnight. Finally, the desired compounds were obtained under vacuum distillation.

4.5. General procedure for the synthesis of compounds (6a-1; 6b-1)

The compounds (**5a-1** or **5b-1**; 1.0 equiv) were dissolved into methanol solution (10 mL), the solution of 2N sodium hydroxide (20 mL) was added. Then, the reaction mixture was stirred at 60 °C for 7 h. The reaction process was monitored by TLC analysis. After the completion of reaction, the methanol solution was removed under vacuum distillation, pH was adjusted to 2-3 by dilute hydrochloric acid solution, and the white solid was filtered and dried to give the desired compounds.

4.6. General procedure for the synthesis of target compounds (7a-1, 2, 3, 4 and 7b-1, 2, 3, 4)

The key intermediate (**6a-1** or **6b-1**; 1.0 equiv) and HATU (1.2 equiv) were added into DMF, respectively. The mixture was stirred at room temperature for 2 h. The 4-aminopyridine, 3-aminopyridine, 4-pyridinemethaneamine or 3-pyridinylmethyl amine (1.2 equiv) and DIEA (2.0 equiv) were added, and the mixture was heated at 80 °C for 7 h. The reaction process was monitored by TLC analysis. After the completion of reaction, the reaction mixture was poured into ice water, and extracted with ethyl acetate, the organic phase was dried by Na_2SO_4 overnight, and the solvent was removed under vacuum. The resulting solid was dried to give the desired compounds. The crude product was purified by silica gel column chromatography (CH_2Cl_2: MeOH =100:3).

4.7. General procedure for the synthesis of target compounds (8a; 8b)

The intermediates (**4a-4** or **4b-4**; 1.0 equiv), CDI (1.2 equiv.) and imidazole (1.0 equiv.) were added to acetonitrile. The mixture was heated at 70 °C for 2 h, and then cooled to room temperature. The solvent was removed under vacuum. The residue was dissolved in ethyl acetate, washed with water thrice, dried over Na_2SO_4 and filtered. The filtrate was concentrated to afford the target compounds (**8a, 8b**) as a white solid. The crude product was purified by silica gel column chromatography (CH_2Cl_2: MeOH =100:3).

4.8. General procedure for the synthesis of key intermediate compounds (9a; 9b)

The compounds (**8a** or **8b**; 1.0 equiv) were dissolved into methanol solution (10 mL), the solution of 2N sodium hydroxide (20 mL) was added. Then, the reaction mixture was stirred at 60 °C for 2 h. The reaction process was monitored by TLC analysis. After the completion of reaction, the methanol solution was removed under vacuum distillation, pH was adjusted to 2-3 by dilute hydrochloric acid solution, and white solid was filtered and dried to give the desired compounds.

4.9. General procedure for the synthesis of key intermediate compounds (10a-1, 2, 3, 4, 5; 10b-1, 2, 3, 4, 5)

The appropriate key intermediate organic acid (**9a** or **9b**;1 equiv) and HATU (1.2 equiv) were added into anhydrous DMF, respectively. The mixture was stirred at room temperature for 2 h. Then, amino intermediates (1.1 equiv) and DIEA (3.0 equiv) were added, the mixed solution was heated at 80 °C for 6 h. The reaction process was monitored by TLC analysis. After the completion of reaction, the reaction mixture was poured into ice water, and extracted with ethyl acetate, the organic phase was dried over Na_2SO_4 overnight. Finally, the desired compounds were obtained under vacuum distillation.

4.10. General procedure for the synthesis of key intermediate compounds (11a-1, 2, 3; 11b-1, 2, 3; 6a-1; 6b-1)

The intermediates (**4a-1, 2, 3, 4** or **4b-1, 2, 3, 4**; 1.0 equiv) were dissolved into methanol solution (10 mL), the solution of 2N sodium hydroxide (20 mL) was added. Then, the reaction mixture was stirred at 60 °C for 7 h. The reaction process was monitored by TLC analysis. After the completion of reaction, the methanol solution was removed under vacuum distillation, pH was adjusted to 2-3 by dilute hydrochloric acid solution, and white solid was filtered and dried to give the desired compounds **(11a-1, 2,**

3; 11b-1, 2, 3; 6a-1; 6b-1).

4.11. General procedure for the synthesis of key intermediates (13a-1, 2, 3; 13b-1, 2, 3; 14a; 14b)

The appropriate key intermediate organic acids (**11a-1, 2, 3; 11b-1, 2, 3; 6a-1; 6b-1**; 1 equiv) and HATU (1.2 equiv) were added into anhydrous DMF, respectively. The mixture was stirred at room temperature for 2 h. Then, aminoacetophenone (1.1 equiv) and DIEA (3.0 equiv) were added, the mixed solution was heated at 80 °C for 6 h. The reaction process was monitored by TLC analysis. After the completion of reaction, the reaction mixture was poured into ice water, and extracted with ethyl acetate, the organic phase was dried over Na_2SO_4 overnight. Finally, the desired compounds were obtained under vacuum distillation.

4.12. General procedure for the synthesis of key intermediates (15a-1, 2, 3; 15b-1, 2, 3; 16a; 16b)

To a solution of the key intermediate compounds (**13a-1, 2, 3; 13b-1, 2, 3; 14a; 14b;** 1.0 equiv) in ethanol, $NaHCO_3$ (0.5 equiv) and 37% formaldehyde solution (1.5 equiv) were added. The mixture was stirred at 50 °C for 48h, and then the organic solvent was removed under vacuum. The residue was dissolved in DCM and washed with water, brine sequentially. The organic phase was dried over Na_2SO_4 and filtered. The filtrate was concentrated and purified by silica column to give the compounds (**15a-1, 2, 3; 15b-1, 2, 3; 16a; 16b)** as a white solid.

4.13. General procedure for the synthesis of target compounds (17a-1, 2, 3; 17b-1, 2, 3; 18a; 18b)

The intermediates (**15a-1, 2, 3; 15b-1, 2, 3; 16a; 16b;** 1.0 equiv), CDI (1.2 equiv.) and imidazole (1.0 equiv) were added to acetonitrile. The mixture was heated at 70 °C for 2 h and then cooled to room temperature. The solvent was removed under vacuum. The residue was dissolved in ethyl acetate, washed with water thrice, dried over Na_2SO_4 and filtered. The filtrate was concentrated to afford the target compounds (**17a-1, 2, 3; 17b-1, 2, 3; 18a; 18b**) as a white solid. The crude product was purified by silica gel column chromatography (CH_2Cl_2: MeOH =100:3).

4.13.1. N-methyl-N-(2-oxo-2-(pyridin-4-ylamino)ethyl)-1-naphthamide (7a-1)

The product was obtained as a white solid; yield: 76.1%; mp: 155.2–157.9°C. ^{1}H NMR (500 MHz, DMSO) δ 10.97 (s, 1H), 8.48 (d, J = 6.0 Hz, 1H), 8.38 (d, J = 6.1 Hz, 1H), 8.11 (d, J = 8.2 Hz, 1H), 8.01 (d, J = 8.1 Hz, 2H), 7.68 (d, J = 6.1 Hz, 2H), 7.62 – 7.57 (m, 2H), 7.48 (d, J = 6.9 Hz, 1H), 7.45 (d, J = 6.1 Hz, 1H), 3.17 (s, 2H), 2.82 (s, 3H). ^{13}C NMR (126 MHz, DMSO) δ 170.76, 168.73, 150.94, 150.83, 146.01, 134.91, 133.39, 129.30, 128.77, 127.50, 126.97, 125.89, 125.53, 124.18, 113.70, 113.60, 50.92, 38.38. ESI-MS m/z: 318 $[M-H]^+$; 320 $[M+H]^+$; 342 $[M+Na]^+$. HPLC purity 98.4%. Retention time: 5.550 min, eluted with 20% purified water/80% methanol.

4.13.2. N-methyl-N-(2-oxo-2-(pyridin-3-ylamino)ethyl)-1-naphthamide (7a-2)

The product was obtained as a white solid; yield: 75.3%; mp: 161.5–164.1°C. ^{1}H NMR (500 MHz, DMSO) δ 10.96 (s, 1H), 8.89 (d, J = 2.0 Hz, 1H), 8.66 (d, J = 2.1 Hz, 1H),

8.30 (d, J = 4.6 Hz, 1H), 8.12 (d, J = 8.2 Hz, 1H), 8.01 (d, J = 8.1 Hz, 2H), 7.71 – 7.54 (m, 4H), 7.42 – 7.39 (m, 1H), 3.17 (s, 2H), 2.82 (s, 3H). ^{13}C NMR (126 MHz, DMSO) δ 170.71, 168.07, 144.67, 141.21, 136.21, 135.00, 133.38, 129.26, 128.75, 127.48, 126.95, 126.53, 125.89, 125.57, 124.15, 50.65, 38.33. ESI-MS m/z: 318 $[M-H]^+$; 320 $[M+H]^+$; 342 $[M+Na]^+$. HPLC purity 99.1%. Retention time: 5.823 min, eluted with 20% purified water/80% methanol.

4.13.3. N-methyl-N-(2-oxo-2-((pyridin-4-ylmethyl)amino)ethyl)-1-naphthamide (7a-3)

The product was obtained as a white solid; yield: 72.4%; mp: 158.2–165.3°C. ^{1}H NMR (500 MHz, DMSO) δ 8.74 (t, *J* = 6.0 Hz, 1H), 8.52 (d, *J* = 5.8 Hz, 1H), 8.45 (d, *J* = 5.7 Hz, 1H), 8.12 – 8.06 (m, 1H), 8.02 – 7.98 (m, 2H), 7.60 – 7.54 (m, 2H), 7.34 (d, *J* = 5.5 Hz, 1H), 7.02 (d, *J* = 5.4 Hz, 1H), 4.44 (d, *J* = 5.9 Hz, 2H), 3.16 (s, 2H), 2.78 (s, 3H). ^{13}C NMR (126 MHz, DMSO) δ 170.62, 168.98, 149.99, 149.91, 148.89, 135.06, 133.36, 129.22, 128.71, 127.39, 126.92, 125.85, 124.17, 122.58, 122.43, 53.51, 50.08, 38.36. ESI-MS m/z: 332 $[M-H]^+$; 334 $[M+H]^+$; 356 $[M+Na]^+$. HPLC purity 98.8%. Retention time: 4.930 min, eluted with 20% purified water/80% methanol.

4.13.4. N-methyl-N-(2-oxo-2-((pyridin-3-ylmethyl)amino)ethyl)-1-naphthamide (7a-4)

The product was obtained as a white solid; yield: 72.6%; mp: 162.2–166.7°C. ^{1}H NMR (500 MHz, DMSO) δ 8.69 (t, *J* = 5.8 Hz, 1H), 8.56 (d, *J* = 1.5 Hz, 1H), 8.48 (dd, *J* = 4.7, 1.3 Hz, 1H), 8.11 – 8.06 (m, 1H), 7.99 (d, *J* = 8.7 Hz, 2H), 7.74 (d, *J* = 7.9 Hz, 2H), 7.58 (s, 1H), 7.46 (d, *J* = 7.1 Hz, 2H), 7.38 (d, *J* = 3.1 Hz, 1H), 4.43 (d, *J* = 5.8 Hz, 2H), 3.14 (s, 2H), 2.77 (s, 3H). ^{13}C NMR (126 MHz, DMSO) δ 170.58, 168.75, 149.21, 149.16, 148.60, 135.55, 135.09, 133.36, 129.48, 129.20, 128.70, 127.40, 126.92, 125.67, 123.96, 123.88, 53.54, 50.02, 38.31. ESI-MS m/z: 332 $[M-H]^+$; 334 $[M+H]^+$; 356 $[M+Na]^+$. HPLC purity 99.0%. Retention time: 5.005 min, eluted with 20% purified water/80% methanol.

4.13.5. N-methyl-N-(2-oxo-2-(pyridin-4-ylamino)ethyl)-2-naphthamide(7b-1)

The product was obtained as a white solid; yield: 72.3%; mp: 156.8–160.5°C. ^{1}H NMR (500 MHz, $CDCl_3$) δ 9.50 (s, 1H), 8.68 (s, 1H), 8.32 (dd, *J* = 4.7, 1.0 Hz, 1H), 8.10 (d, *J* = 8.0 Hz, 1H), 8.01 (s, 1H), 7.92 – 7.85 (m, 3H), 7.56 (s, 3H), 7.22 (dd, *J* = 8.3, 4.8 Hz, 1H), 4.36 (s, 2H), 3.21 (s, 3H). ^{13}C NMR (126 MHz, $CDCl_3$) δ 173.19, 167.53, 145.13, 141.30, 134.91, 134.05, 132.51, 131.61, 128.54, 127.86, 127.75, 127.62, 126.99, 124.21, 123.62, 53.69, 39.61. ESI-MS m/z: 318 $[M-H]^+$; 320 $[M+H]^+$; 342 $[M+Na]^+$. HPLC purity 98.9%. Retention time: 5.947 min, eluted with 20% purified water/80% methanol.

4.13.6. N-methyl-N-(2-oxo-2-(pyridin-3-ylamino)ethyl)-2-naphthamide(7b-2)

The product was obtained as a white solid; yield: 79.4%; mp: 163.7–168.2°C. ^{1}H NMR (500 MHz, $CDCl_3$) δ 9.53 (s, 1H), 8.68 (s, 1H), 8.31 (dd, *J* = 4.9, 1.0 Hz, 1H), 8.11 (d, *J* = 9.3 Hz, 1H), 8.03 (s, 1H), 7.92 – 7.87 (m, 3H), 7.56 (s, 3H), 7.18 (dd, *J* = 8.6, 4.9 Hz, 1H), 4.38 (s, 2H), 3.23 (s, 3H). ^{13}C NMR (126 MHz, $CDCl_3$) δ 172.32, 167.28, 145.55, 140.74, 128.80, 127.87, 127.65, 123.50, 123.35, 122.89, 122.32, 122.20, 121.88, 121.55, 119.46, 52.07, 41.22. ESI-MS m/z: 318 $[M-H]^+$; 320 $[M+H]^+$; 342 $[M+Na]^+$. HPLC purity 99.3%. Retention time: 5.671 min, eluted with 20% purified water/80% methanol.

4.13.7. N-methyl-N-(2-oxo-2-((pyridin-4-ylmethyl)amino)ethyl)-2-naphthamide(7b-3)

The product was obtained as a white solid; yield: 71.9%; mp: 161.8–166.2°C. ^{1}H NMR (500 MHz, DMSO) δ 8.51 (d, *J* = 20.1 Hz, 3H), 7.96 – 7.84 (m, 3H), 7.71 (s, 1H), 7.62 – 7.48 (m, 3H), 7.30 (s, 1H), 7.16 (s, 1H), 4.44 (d, *J* = 38.4 Hz, 2H), 4.01 (s, 1H), 3.15 (s, 3H). ^{13}C NMR (126 MHz, HDMSO) δ 171.80, 168.98, 149.69, 148.45, 133.60, 133.12, 132.51, 128.39, 127.83, 127.21, 126.81, 126.33, 124.56, 124.33, 122.44, 54.50, 51.05, 38.60. ESI-MS m/z: 332 $[M-H]^+$; 334 $[M+H]^+$; 356 $[M+Na]^+$. HPLC purity 98.5%. Retention time: 5.011 min, eluted with 20% purified water/80% methanol.

4.13.8. N-methyl-N-(2-oxo-2-((pyridin-3-ylmethyl)amino)ethyl)-2-naphthamide(7b-4)

The product was obtained as a white solid; yield: 77.4%; mp: 169.4–173.0°C. ^{1}H NMR (500 MHz, DMSO) δ 8.50 (d, *J* = 16.4 Hz, 3H), 7.90 – 7.86 (m, 3H), 7.73 (s, 1H), 7.57 – 7.52 (m, 3H), 7.38 (s, 1H), 7.15 (s, 1H), 4.46 (d, *J* = 27.6 Hz, 2H), 4.06 (s, 1H), 3.13 (s, 3H). ^{13}C NMR (126 MHz, HDMSO) δ 172.26, 168.79, 149.86, 148.12, 136.42, 133.67, 133.52, 133.12, 132.53, 131.92, 128.49, 128.33, 128.10, 127.83, 127.69, 127.28, 127.06, 126.33, 124.38, 122.75, 54.23, 50.55, 39.29. ESI-MS m/z: 332 $[M-H]^+$; 334 $[M+H]^+$; 356 $[M+Na]^+$. HPLC purity 99.5%. Retention time: 5.150 min, eluted with 20% purified water/80% methanol.

4.13.9.N-(1-(cyclohexylamino)-3-(1H-imidazol-1-yl)-1-oxopropan-2-yl)-1-naphthamide (10a-1)

The product was obtained as a white solid; yield: 70.8%; mp: 132.6–138.1°C. ^{1}H NMR (500 MHz, DMSO) δ 8.79 (d, *J* = 8.5 Hz, 1H), 8.07 (d, *J* = 7.7 Hz, 1H), 8.01 (d, *J* = 8.2 Hz, 1H), 7.96 (d, *J* = 8.6 Hz, 2H), 7.62 (s, 1H), 7.57 – 7.45 (m, 4H), 7.20 (s, 1H), 6.92 (s, 1H), 4.92 (td, *J* = 9.4, 4.8 Hz, 1H), 4.29 (ddd, *J* = 23.7, 13.9, 7.3 Hz, 2H), 3.69 – 3.51 (m, 1H), 1.87 – 1.66 (m, 4H), 1.33 – 1.12 (m, 6H). ^{13}C NMR (126 MHz, DMSO) δ 169.09, 168.27, 138.27, 134.58, 133.52, 130.46, 130.11, 128.74, 128.57, 127.12, 126.72, 125.86, 125.73, 125.37, 120.26, 54.72, 48.28, 47.63, 32.69, 25.65, 24.90. ESI-MS m/z: 389 $[M-H]^+$; 391 $[M+H]^+$; 413 $[M+Na]^+$. HPLC purity 99.5%. Retention time: 5.484 min, eluted with 20% purified water/80% methanol.

4.13.10.N-(1-(cyclopentylamino)-3-(1H-imidazol-1-yl)-1-oxopropan-2-yl)-1-naphthamide (10a-2)

The product was obtained as a white solid; yield: 69.5%; mp: 137.2–140.3°C. ^{1}H NMR (500 MHz, DMSO) δ 8.78 (d, *J* = 8.9 Hz, 1H), 8.24 (d, *J* = 11.3 Hz, 1H), 8.03 – 7.95 (m, 3H), 7.64 (s, 1H), 7.56 – 7.47 (m, 4H), 7.21 (s, 1H), 6.94 (s, 1H), 4.91 (td, *J* = 7.5, 6.2 Hz, 1H), 4.29 (ddd, *J* = 18.6, 12.7, 9.8 Hz, 2H), 4.10 – 4.01 (m, 1H), 1.85 – 1.46 (m, 8H). ^{13}C NMR (126 MHz, DMSO) δ 166.03, 163.99, 139.83, 135.61, 133.37, 130.21, 129.43, 128.02, 127.71, 127.52, 123.90, 119.84, 53.77, 52.03, 47.46, 32.67, 32.54, 24.74. ESI-MS m/z: 375 $[M-H]^+$; 377 $[M+H]^+$; 399 $[M+Na]^+$. HPLC purity 99.3%. Retention time: 5.004 min, eluted with 20% purified water/80% methanol.

4.13.11.N-(1-(benzylamino)-3-(1H-imidazol-1-yl)-1-oxopropan-2-yl)-1-naphthamide (10a-3)

The product was obtained as a white solid; yield: 65.3%; mp: 141.6–145.8°C. ^{1}H NMR (500 MHz, DMSO) δ 8.97 (d, *J* = 9.8 Hz, 1H), 8.75 (t, *J* = 7.3 Hz, 1H), 8.48 (s, 1H), 8.03 – 7.99 (m, 3H), 7.93 – 7.86 (m, 1H), 7.78 (s, 1H), 7.65 – 7.63 (m, 2H), 7.31 – 7.24 (m, 6H), 6.84 (s, 1H), 4.99 (td, *J* = 11.4, 6.8 Hz, 1H), 4.42 – 4.40 (m, 2H), 4.36 (t, *J* = 7.9 Hz, 2H). ^{13}C NMR (126 MHz, DMSO) δ 170.19, 167.98, 140.01, 138.61, 135.45, 133.00, 130.94, 129.54, 129.15, 128.47, 128.06, 127.48, 127.04, 124.07, 120.75, 55.66, 48.23, 44.51. ESI-MS m/z: 397 $[M-H]^+$; 399 $[M+H]^+$; 421 $[M+Na]^+$. HPLC purity 99.1%. Retention time: 5.108 min, eluted with 20% purified water/80% methanol.

4.13.12.*N-(3-(1H-imidazol-1-yl)-1-oxo-1-(p-tolylamino)propan-2-yl)-1-naphthamide (10a-4)*

The product was obtained as a white solid; yield: 54.9%; mp: 137.6–143.9°C. ^{1}H NMR (500 MHz, DMSO) δ 8.96 (d, *J* = 5.9 Hz, 1H), 8.77 (t, *J* = 6.3 Hz, 1H), 8.46 (s, 1H), 8.05 – 8.03 (m, 3H), 7.97 – 7.83 (m, 1H), 7.73 (s, 1H), 7.62 (dd, *J* = 9.9, 3.9 Hz, 2H), 7.37 (t, *J* = 7.4 Hz, 2H), 7.23 (dd, *J* = 15.1, 5.7 Hz, 4H), 6.91 (s, 1H), 4.99 (td, *J* = 9.7, 4.5 Hz, 1H), 4.54 – 4.38 (m, 2H), 1.23 (s, 1H). ^{13}C NMR (126 MHz, DMSO) δ 170.54, 166.43, 140.06, 137.16, 136.37, 133.12, 131.18, 130.65, 129.33, 128.76, 128.31, 128.23, 128.11, 127.65, 127.30, 124.13, 119.80, 56.05, 48.66, 29.27. ESI-MS m/z: 399 $[M+H]^+$; 421 $[M+Na]^+$. HPLC purity 99.3%. Retention time: 5.108 min, eluted with 20% purified water/80% methanol.

4.13.13.N-(3-(1H-imidazol-1-yl)-1-oxo-1-((pyridin-4-ylmethyl)amino)propan-2-yl)-1-naphthamide (10a-5)

The product was obtained as a white solid; yield: 72.7%; mp: 145.2–149.6°C. ^{1}H NMR (500 MHz, DMSO) δ 8.91 (d, *J* = 7.3 Hz, 1H), 8.72 (t, *J* = 6.8 Hz, 1H), 8.42 (s, 1H), 8.00 – 7.97 (m, 3H), 7.89 (d, *J* = 7.4 Hz, 1H), 7.75 (s, 1H), 7.56 (m, 2H), 7.28 – 7.22 (m, 4H), 7.02 (s, 1H), 6.84 (s, 1H), 4.94 (td, *J* = 9.7, 4.5 Hz, 1H), 4.53 – 4.36 (m, 2H), 4.07 (s, 3H). ^{13}C NMR (126 MHz, DMSO) δ 169.99, 164.28, 145.49, 142.31, 139.98, 135.36, 133.93, 131.07, 128.74, 127.91, 127.29, 124.69, 120.36, 117.48, 56.59, 51.70, 47.99. ESI-MS m/z: 400 $[M+H]^+$; 422 $[M+Na]^+$. HPLC purity 99.3%. Retention time: 5.108 min, eluted with 20% purified water/80% methanol.

4.13.14.N-(1-(cyclohexylamino)-3-(1H-imidazol-1-yl)-1-oxopropan-2-yl)-2-naphthamide (10b-1)

The product was obtained as a white solid; yield: 70.2%; mp: 131.6–135.4°C.^{1}H NMR (500 MHz, DMSO) δ 8.84 (d, *J* = 8.5 Hz, 1H), 8.45 (s, 1H), 8.11 (d, *J* = 7.8 Hz, 1H), 8.07 – 7.95 (m, 4H), 7.90 (dd, *J* = 8.6, 1.5 Hz, 1H), 7.62 (td, *J* = 7.2, 1.3 Hz, 2H), 7.31 (s, 1H), 7.02 (s, 1H), 4.93 (td, *J* = 9.1, 4.9 Hz, 1H), 4.41 (ddd, *J* = 23.5, 13.9, 7.3 Hz, 2H), 3.58 – 3.54 (m, 1H), 1.79 – 1.65 (m, 4H), 1.32 – 1.12 (m, 6H). ^{13}C NMR (126 MHz, DMSO) δ 168.20, 166.89, 137.79, 134.73, 132.51, 131.48, 129.35, 128.34, 128.29, 128.25, 128.11, 127.29, 124.69, 120.94, 54.68, 48.33, 48.23, 32.68, 32.65, 25.63, 24.98. ESI-MS m/z: 389 $[M-H]^+$; 391 $[M+H]^+$; 413 $[M+Na]^+$. HPLC purity 99.6%. Retention time: 5.484 min, eluted with 20% purified water/80% methanol.

4.13.15.N-(1-(cyclopentylamino)-3-(1H-imidazol-1-yl)-1-oxopropan-2-yl)-2-naphthami

de (10b-2)

The product was obtained as a white solid; yield: 67.2%; mp: 137.6–141.8°C. ^{1}H NMR (500 MHz, DMSO) δ 8.77 (d, *J* = 8.5 Hz, 1H), 8.14 (d, *J* = 7.1 Hz, 1H), 8.01 (d, *J* = 8.1 Hz, 1H), 7.96 (dd, *J* = 7.7, 5.2 Hz, 2H), 7.62 (s, 1H), 7.53 (ddd, *J* = 22.4, 13.2, 2.4 Hz, 4H), 7.19 (s, 1H), 6.92 (s, 1H), 4.92 (td, *J* = 9.5, 4.8 Hz, 1H), 4.29 (ddd, *J* = 23.7, 13.9, 7.3 Hz, 2H), 4.06 (dd, *J* = 13.4, 6.5 Hz, 1H), 1.89 – 1.51 (m, 8H). ^{13}C NMR (126 MHz, DMSO) δ 168.66, 166.87, 137.88, 134.72, 132.51, 131.50, 129.35, 128.34, 128.28, 128.11, 127.29, 124.69, 120.75, 54.66, 51.01, 48.07, 32.67, 32.54, 23.95, 23.92. ESI-MS m/z: 375 $[M-H]^+$; 377 $[M+H]^+$; 399 $[M+Na]^+$. HPLC purity 99.4%. Retention time: 5.583 min, eluted with 20% purified water/80% methanol.

4.13.16.N-(1-(benzylamino)-3-(1H-imidazol-1-yl)-1-oxopropan-2-yl)-2-naphthamide (10b-3)

The product was obtained as a white solid; yield: 69.4%; mp: 143.6–148.3°C. ^{1}H NMR (500 MHz, DMSO) δ 8.95 (d, *J* = 8.5 Hz, 1H), 8.74 (t, *J* = 5.9 Hz, 1H), 8.45 (s, 1H), 8.15 – 7.95 (m, 3H), 7.94 – 7.81 (m, 1H), 7.75 (s, 1H), 7.69 – 7.51 (m, 2H), 7.43 – 7.17 (m, 6H), 6.87 (s, 1H), 4.97 (td, *J* = 9.7, 4.5 Hz, 1H), 4.60 – 4.25 (m, 4H). ^{13}C NMR (126 MHz, DMSO) δ 169.50, 167.05, 139.50, 138.12, 134.72, 132.49, 131.55, 129.33, 128.76, 128.31, 128.23, 128.11, 127.65, 127.30, 124.75, 120.43, 55.08, 47.53, 42.76. ESI-MS m/z: 399 $[M+H]^+$; 421 $[M+Na]^+$. HPLC purity 99.2%. Retention time: 5.350 min, eluted with 20% purified water/80% methanol.

4.13.17.N-(3-(1H-imidazol-1-yl)-1-oxo-1-(p-tolylamino)propan-2-yl)-2-naphthamide (10b-4)

The product was obtained as a white solid; yield: 50.4%; mp: 143.6–148.3°C. ^{1}H NMR (500 MHz, DMSO) δ 8.96 (d, *J* = 9.2 Hz, 1H), 8.79 (d, *J* = 7.9 Hz, 1H), 8.46 (s, 1H), 8.06 – 7.95 (m, 4H), 7.82 – 7.71 (m, 1H), 7.62 (s, 1H), 7.54 (ddd, *J* = 30.5, 14.8, 4.8 Hz, 5H), 7.22 (s, 1H), 6.94 (s, 1H), 4.94 (td, *J* = 9.4, 4.8 Hz, 1H), 4.28 (ddd, *J* = 23.7, 13.9, 7.3 Hz, 2H), 1.15 (s, 3H). ^{13}C NMR (126 MHz, DMSO) δ 170.36, 167.76, 140.40, 138.56, 135.71, 133.14, 131.23, 128.76, 128.31, 128.23, 127.65, 127.30, 121.30, 56.76, 48.75, 31.07. ESI-MS m/z: 399 $[M+H]^+$; 421 $[M+Na]^+$. HPLC purity 99.2%. Retention time: 5.034 min, eluted with 20% purified water/80% methanol.

4.13.18.N-(3-(1H-imidazol-1-yl)-1-oxo-1-((pyridin-4-ylmethyl)amino)propan-2-yl)-2-naphthamide(10b-5)

The product was obtained as a white solid; yield: 66.1%; mp: 146.2–150.6°C. ^{1}H NMR (500 MHz, DMSO) δ 8.82 (d, *J* = 5.9 Hz, 1H), 8.45 (d, *J* = 8.1 Hz, 1H), 8.17 (d, *J* = 6.2 Hz, 1H), 7.98 – 7.93 (m, 3H), 7.79 (s, 1H), 7.62 (d, *J* = 8.1Hz, 1H),7.52 (ddd, *J* = 13.5, 9.8, 7.8 Hz, 5H), 7.19 (s, 1H), 6.87 (s, 1H), 4.94 (td, *J* = 9.4, 4.8 Hz, 1H), 4.26 (ddd, *J* = 17.3, 10.5, 5.8 Hz, 2H), 4.05 (s, 3H). ^{13}C NMR (126 MHz, DMSO) δ 170.31, 165.70, 141.48, 137.11, 136.06, 135.67, 133.68, 133.12, 131.08, 129.63, 128.23, 128.11, 127.91, 127.30, 125.56, 123.53, 122.01, 118.39, 56.59, 48.83, 43.37. ESI-MS m/z: 400 $[M+H]^+$; 422 $[M+Na]^+$. HPLC purity 99.4%. Retention time: 4.124 min, eluted with 20% purified water/80% methanol.

4.13.19.N-(2-((3-(1H-imidazol-1-yl)-1-oxo-1-phenylpropan-2-yl)amino)-2-oxoethyl)-1-naphthamide(17a-1)

The product was obtained as a white solid; yield: 63.7%; mp: 161.2–164.9°C. ^{1}H NMR (500 MHz, DMSO) δ 8.81 – 8.63 (m, 2H), 8.28 – 8.16 (m, 1H), 8.01 (d, *J* = 7.6 Hz, 3H), 7.97 – 7.94 (m, 1H), 7.66 (d, *J* = 7.3 Hz, 1H), 7.61 (d, *J* = 2.2 Hz, 1H), 7.59 – 7.48 (m, 6H), 7.19 (s, 1H), 6.85 (s, 1H), 5.64 (td, *J* = 8.3, 4.7 Hz, 1H), 4.40 (ddd, *J* = 22.6, 14.2, 6.5 Hz, 2H), 3.86 (qd, *J* = 16.3, 6.0 Hz, 2H).^{13}C NMR (126 MHz, DMSO) δ 197.11, 169.42, 169.37, 138.38, 135.15, 134.67, 134.19, 133.58, 130.43, 130.29, 129.24, 128.95, 128.74, 128.54, 127.08, 126.66, 126.20, 125.80, 125.35, 120.58, 54.81, 46.69, 42.82. ESI-MS m/z: 425 $[M-H]^+$; 427 $[M+H]^+$; 449 $[M+Na]^+$. HPLC purity 99.4%. Retention time: 4.841 min, eluted with 20% purified water/80% methanol.

4.13.20.N-(1-((3-(1H-imidazol-1-yl)-1-oxo-1-phenylpropan-2-yl)amino)-1-oxopropan-2-yl)-1-naphthamide(17a-2)

The product was obtained as a white solid; yield: 72.5%; mp: 165.2–169.1°C. ^{1}H NMR (500 MHz, DMSO) δ 8.86 (d, *J* = 8.5 Hz, 1H), 8.71 (d, *J* = 8.4 Hz, 1H), 8.62 (d, *J* = 6.9 Hz, 1H), 8.19 – 8.15 (m, 1H), 7.99 (d, *J* = 7.4 Hz, 4H), 7.78 (d, *J* = 7.5 Hz, 1H), 7.54 (d, *J* = 9.9 Hz, 6H), 7.24 (s, 1H), 6.86 (s, 1H), 5.50 (td, *J* = 8.9, 3.9 Hz, 1H), 4.45 (t, *J* = 7.2 Hz, 1H), 4.36 – 4.28 (m, 2H), 1.00 (d, *J* = 7.2 Hz, 3H). ^{13}C NMR (126 MHz, DMSO) δ 197.30, 182.47, 168.98, 138.51, 135.35, 134.74, 133.51, 133.14, 132.54, 130.22, 129.36, 129.12, 128.98, 128.66, 128.53, 127.07, 126.62, 126.06, 125.84, 125.33, 120.68, 55.00, 49.35, 46.40, 17.32. ESI-MS m/z: 441 $[M+H]^+$; 463 $[M+Na]^+$. HPLC purity 98.9%. Retention time: 4.879 min, eluted with 20% purified water/80% methanol.

4.13.21.N-(1-((3-(1H-imidazol-1-yl)-1-oxo-1-phenylpropan-2-yl)amino)-3-methyl-1-oxobutan-2-yl)-1-naphthamide(17a-3)

The product was obtained as a white solid; yield: 69.4%; mp: 168.7–171.5°C. ^{1}H NMR (500 MHz, DMSO) δ 8.90 (d, *J* = 8.4 Hz, 1H), 8.44 (d, *J* = 8.7 Hz, 1H), 7.99 (ddd, *J* = 17.5, 9.2, 8.2 Hz, 5H), 7.63 (d, *J* = 16.6 Hz, 2H), 7.58 – 7.45 (m, 6H), 7.23 (s, 1H), 6.85 (s, 1H), 5.70 (td, *J* = 8.5, 4.6 Hz, 1H), 4.51 (dt, *J* = 14.1, 4.8 Hz, 1H), 4.32 (ddd, *J* = 12.4, 8.5, 5.7 Hz, 2H), 1.95 – 1.82 (m, 1H), 0.82 (d, *J* = 6.7 Hz, 6H). ^{13}C NMR (126 MHz, DMSO) δ 197.19, 171.38, 168.98, 138.42, 135.28, 134.98, 134.14, 133.63, 133.51, 130.24, 129.15, 129.02, 128.91, 128.66, 128.55, 127.09, 126.62, 125.96, 125.77, 125.35, 120.49, 59.19, 54.68, 46.73, 30.58, 19.50. ESI-MS m/z: 467 $[M-H]^+$; 469 $[M+H]^+$; 491 $[M+Na]^+$. HPLC purity 99.2%. Retention time: 5.991 min, eluted with 20% purified water/80% methanol.

4.13.22.N-(2-((3-(1H-imidazol-1-yl)-1-oxo-1-phenylpropan-2-yl)amino)-2-oxoethyl)-2-naphthamide (17b-1)

The product was obtained as a white solid; yield: 69.1%; mp: 159.3–164.8°C. ^{1}H NMR (500 MHz, DMSO) δ 8.91 (d, *J* = 5.7 Hz, 1H), 8.74 (d, *J* = 8.3 Hz, 1H), 8.47 (s, 1H), 7.99 (dt, *J* = 17.0, 8.0 Hz, 6H), 7.68 – 7.57 (m, 4H), 7.53 (t, *J* = 7.7 Hz, 2H), 7.22 (s, 1H), 6.88 (s, 1H), 5.58 (td, *J* = 8.3, 4.7 Hz, 1H), 4.53 – 4.23 (m, 2H), 3.86 (ddd, *J* = 42.1, 16.5, 5.9 Hz, 2H). ^{13}C NMR (126 MHz, DMSO) δ 197.09, 169.52, 167.04, 135.19, 134.67, 134.15,

132.57, 131.74, 129.34, 129.22, 128.91, 128.29, 128.20, 128.13, 128.09, 127.22, 124.68, 54.82, 43.05, 21.53. ESI-MS m/z: 425 $[M-H]^+$; 427 $[M+H]^+$; 449 $[M+Na]^+$. HPLC purity 99.4%. Retention time: 5.108 min, eluted with 20% purified water/80% methanol.

4.13.23.N-(1-((3-(1H-imidazol-1-yl)-1-oxo-1-phenylpropan-2-yl)amino)-1-oxopropan-2-yl)-2-naphthamide(17b-2)

The product was obtained as a white solid; yield: 70.5%; mp: 165.2–169.7°C. ^{1}H NMR (500 MHz, DMSO) δ 8.83 (d, *J* = 8.3 Hz, 1H), 8.59 (d, *J* = 7.0 Hz, 1H), 8.48 (s, 1H), 8.07 – 8.01 (m, 1H), 8.00 – 7.88 (m, 4H), 7.66 (s, 1H), 7.64 – 7.56 (m, 4H), 7.50 (t, *J* = 7.7 Hz, 2H), 7.23 (s, 1H), 6.87 (s, 1H), 5.45 (td, *J* = 8.9, 4.2 Hz, 1H), 4.54 (dd, *J* = 14.1, 4.1 Hz, 1H), 4.41 – 4.22 (m, 2H), 1.09 (d, *J* = 7.2 Hz, 3H). ^{13}C NMR (126 MHz, DMSO) δ 197.47, 172.84, 166.67, 138.49, 135.62, 135.40, 134.64, 133.84, 132.54, 131.75, 129.30, 128.97, 128.91, 128.64, 128.26, 128.14, 128.07, 127.16, 124.92, 120.70, 55.22, 49.52, 46.44, 17.58. ESI-MS m/z: 439 $[M-H]^+$; 441 $[M+H]^+$; 463 $[M+Na]^+$. HPLC purity 98.9%. Retention time: 5.437 min, eluted with 20% purified water/80% methanol.

4.13.24.N-(1-((3-(1H-imidazol-1-yl)-1-oxo-1-phenylpropan-2-yl)amino)-3-methyl-1-oxobutan-2-yl)-2-naphthamide(17b-3)

The product was obtained as a white solid; yield: 69.5%; mp: 168.7–173.2°C. ^{1}H NMR (500 MHz, DMSO) δ 8.97 (d, *J* = 4.7 Hz, 1H), 8.62 (d, *J* = 8.3 Hz, 1H), 8.44 (d, *J* = 8.8 Hz, 2H), 8.04 (d, *J* = 7.4 Hz, 1H), 7.98 (dd, *J* = 12.1, 6.5 Hz, 4H), 7.77 (d, *J* = 7.6 Hz, 1H), 7.62 (dd, *J* = 8.7, 6.1 Hz, 5H), 7.20 (s, 1H), 7.15 (s, 1H), 5.53 (ddd, *J* = 14.7, 9.4, 5.1 Hz, 1H), 4.62 – 4.42 (m, 1H), 4.28 (dt, *J* = 16.3, 6.6 Hz, 2H), 2.17 (dt, *J* = 13.5, 6.8 Hz, 1H), 0.93 (d, *J* = 6.7 Hz, 6H). ^{13}C NMR (126 MHz, DMSO) δ 192.06, 171.43, 166.96, 141.13, 138.36, 136.56, 135.34, 134.62, 133.98, 133.12, 132.52, 131.79, 129.39, 129.31, 129.00, 128.20, 128.08, 127.13, 125.02, 120.48, 54.94, 54.59, 46.24, 30.23, 19.50, 19.30. ESI-MS m/z: 467 $[M-H]^+$; 469 $[M+H]^+$; 491 $[M+Na]^+$. HPLC purity 99.4%. Retention time: 6.232 min, eluted with 20% purified water/80% methanol.

4.13.25.N-(2-((3-(1H-imidazol-1-yl)-1-oxo-1-phenylpropan-2-yl)amino)-2-oxoethyl)-N-methyl-1-naphthamide(18a)

The product was obtained as a white solid; yield: 66.8%; mp: 161.5–166.4°C. ^{1}H NMR (500 MHz, DMSO) δ 8.91 (d, *J* = 8.4 Hz, 1H), 8.03 (d, *J* = 7.5 Hz, 1H), 8.00 – 7.96 (m, 2H), 7.66 (d, *J* = 8.5 Hz, 4H), 7.63 (s, 1H), 7.55 (dd, *J* = 11.1, 5.7 Hz, 5H), 7.22 (s, 1H), 7.03 (s, 1H), 5.80 – 5.67 (m, 1H), 4.58 – 4.37 (m, 2H), 3.97 (s, 2H), 2.56 (s, 3H). ^{13}C NMR (126 MHz, DMSO) δ 197.16, 170.40, 168.49, 138.41, 135.61, 135.15, 134.24, 133.34, 129.42, 129.26, 128.94, 128.71, 127.41, 126.91, 125.56, 124.17, 122.13, 120.61, 54.74, 49.59, 46.75, 37.74. ESI-MS m/z: 439 $[M-H]^+$; 441 $[M+H]^+$; 463 $[M+Na]^+$. HPLC purity 99.4%. Retention time: 6.328 min, eluted with 20% purified water/80% methanol.

4.13.26.N-(2-((3-(1H-imidazol-1-yl)-1-oxo-1-phenylpropan-2-yl)amino)-2-oxoethyl)-N-methyl-2-naphthamide(18b)

The product was obtained as a white solid; yield: 68.5%; mp: 164.8–169.2°C.^{1}H NMR (500 MHz, DMSO) δ 8.61 (d, *J* = 16.5 Hz, 1H), 8.02 (d, *J* = 7.5 Hz, 1H), 7.95 – 7.92 (m, 2H), 7.67 – 7.59 (m, 5H), 7.57 – 7.53 (m, 5H), 7.27 (s, 1H), 7.16 (s, 1H), 5.73 (dd, *J* =

8.3, 4.8 Hz, 1H), 4.23 (ddd, *J* = 78.1, 14.0, 9.1 Hz, 2H), 3.84 (s, 2H), 2.72 (s, 3H). ^{13}C NMR (126 MHz, DMSO) δ 196.92, 170.62, 168.10, 137.83, 135.44, 135.10, 134.77, 134.09, 133.22, 129.77, 129.20, 128.96, 128.66, 127.57, 126.40, 125.26, 123.51, 121.62, 120.71, 53.40, 48.80, 46.40, 38.16. ESI-MS m/z: 439 $[M-H]^+$; 441 $[M+H]^+$; 463 $[M+Na]^+$. HPLC purity 99.4%. Retention time: 4.842 min, eluted with 20% purified water/80% methanol.

4.14. Ligand preparation and protein structure preparation

Ligand preparation was performed using LigPrep, which included adding all hydrogen atoms, adjusting the bond order and generating the conformations with low energy. Protein structure preparation: The SE homology model and the protein crystals structure of CYP51 (5TZ1) were processed with the protein preparation module in the DS 3.5. The program was performed as follows: Added all hydrogen atoms, optimized the side chain of amino acid residues, completed the loop area and protonated the structure at the specified pH value. At the same time, CHARMm forcefield was assigned to ligand molecule and receptor protein.

4.15. Docking simulations

In order to evaluate the binding modes between active fragments (or target compound **17a-2**) with target enzymes (SE, CYP51), the molecular docking was performed using MCSS (or CDOCKER). First, the binding region of co-crystallized ligand was selected as the active center of target enzyme. The parameter of active sphere was set to 12 Å, the active sites coordinate of SE (-18.929, 72.693, 54.805) and CYP51 (70.589, 66.306, 4.328) were determined. The maximum conformation was set to 10, and all other options were kept as the default settings during the docking process.

4.16. Antifungal activity test in vitro

The antifungal activity of target compounds was tested using the standard guidelines, which described in the National Committee for Clinical Laboratory Standards (NCCLS), and the in *vitro* minimum inhibitory concentrations (MIC_{50}) value was defined as the lowest concentration of antifungal inhibitor with 50% fungus inhibitory effect. Naftifine and fluconazole were selected as positive control drugs. In the study, the pathogenic fungi were cultured using the Sabouraud medium, and the particular fungal solution was added into 24-well culture plate. The different concentration gradient was set to 0.0625, 0.125, 0.5, 1, 2, 4, 8 and 16 μg/mL, respectively. They were serially dripped into the growth medium with different strains. Subsequently, they were statically cultured in the 35 °C incubator, and the MIC_{50} results were observed and recorded.

4.17. The experiment of Transmission Electron Microscopy (TEM)

According to the test protocol of NCCLS, *C.alb.* SC5314 was selected as the test strain. The concentration of target compound **17a-2** in the fungal solution was adjusted to 4 μg/mL, and they were incubated at 35 °C. Subsequently, the bacterial solution was sampled at different time points (72h, 144h), and they were fixed in 4°C refrigerators with 3% glutaric acid, washed with PBS solution. Finally, these samples were further stained with uranium osmium for 30 min, they were observed using transmission electron microscopy.

4.18. The analysis experiment of sterol components for C. alb. cells

In this process, *C.alb.* SC5314 was selected as the test strain. Naftifine and fluconazole were purchased as the positive control drug. In the study, the concentration of target compounds was set to 0.125 μg/mL, 0.5 μg/mL and 4 μg/mL. After 48 hours of cultivation, the different groups of wet bacteria are concentrated and washed with PBS, and the sterol component was extracted using petroleum ether. The solvent was removed under reduced pressure. Finally, the product was dissolved in methanol solution (10 mL), filtered and detected by LC-MS. The chromatographic conditions were selected with Phenomenex Luna C_{18} (2.50 mm×4.6 mm, 5 μm) column. The mobile phase was methanol-water (98:2), the flow rate was 1 mL/min^{-1}, and the detection wavelength was 210 nm. The peak area ratio of each component is calculated.

4.19. The study of dual-target enzyme inhibition

The target enzymes (SE, CYP51) were extracted from *C.alb.* SC5314 by the corresponding enzyme-reagent boxes. The different concentrations of target compounds and 50 μg target enzyme were dissolved in 200 μL buffer (50 mm Tris, pH 7.4, 150 mM KCl, 10 mm $MgCl_2$, 2 mm NADPH, 0.1 μm squalene or eburicol) solution, respectively. They were incubated for 30 min at 37 ℃. Finally, the acetonitrile solution (125 μL) was added to terminate the reaction, the reaction mixture was centrifuged at 10000 g. The CYP51 activity was quantified according to the consumption of substrate. The content of eburicol was detected by HPLC. The substrate (squalene) was treated with sulfuric acid and formaldehyde to produce the yellow complex. The SE activity was quantified according to the consumption of substrate. The detection was carried out by spectrophotometer (400 nm wavelength).

4.20. In vivo Therapeutic Efficacy

First, the fungal infection mouse models was constructed, and *C.alb.* SC5314 was injected into the mouse abdomen by subcutaneous injection. Subsequently, these mouse with abdominal *Candida* infection were randomly divided into three groups: (1) Saline solution-injected group; (2) Compound **10b**-**5**-injected group; (3) Compound **17a-2**-injected group. Therapy was continued through abdominal injection for 7 days. Finally, these mice tissues, including the heart, livers, spleen, lung, kidney, and endothelial tissue in abdominal infection, were harvested and collected immediately for *H/E* histology analysis. All of the animal experiments were conducted under approved protocols of the Institutional Animal Care and Use Committee of Liaocheng University.

4.21. ADME/T prediction

The pharmacokinetic properties and toxicity (ADME/T) are an important index of the drug-forming property of target compounds. In the study, the target compounds were predicted using the DS ADMET program in Discovery Studio 3.5. The specific operation process was performed as follows: Frist, the small molecule compound files containing target compounds were imported. Then, the “ADMET descriptors” module was selected and opened, the prediction items (aqueous solubility, blood brain barrier penetration, CYP2D6 binding, hepatotoxicity, intestinal absorption and plasma protein

binding) were set as research objects in the parameter browser, respectively. Finally, the program was run to obtain the corresponding results.

Declaration of interest

The authors report no declarations of interest.

Acknowledgements

This work was supported by the National Natural Science Foundation of China (Grant No. 81703357, Grant No. 21473085, Grant No.31701827), the Shandong Provincial Natural Science Foundation (Grant No. ZR2017BH102) and the Open Project of Shandong Cllaborative Innovation Center for Antibody Drugs (Grant No. CIC-AD1837and the Open Project of Shandong Collaborative Innovation Center for Antibody Drugs, and Tai-Shan Scholar Research Fund of Shandong Province of China. This work was also technically supported by Engineering Research Center for Nanomedicine and Drug Delivery Systems.

References

[1] G.D. Brown, D.W. Denning, S.M. Levitz, Tackling human fungal infections, Sci. 336 (2012) 647.

[2] N.M. Revie, K.R. Iyer, N. Robbins, L.E. Cowen, Antifungal drug resistance: evolution, mechanisms and impact, Curr. Opin. Microbiol. 45 (2018) 70-76.

[3] J. Nalawade, A. Shinde, A. Chavan, S. Patil, M. Suryavanshi, M. Modak, P. Choudhari, V.D. Bobade, P.C. Mhaske, Synthesis of new thiazolyl-pyrazolyl-1,2,3-triazole derivatives as potential antimicrobial agents, Eur. J. Med. Chem.179 (2019) 649-659.

[4] D.A. Enoch, H. Yang, S.H. Aliyu, C. Micallef, The changing epidemiology of invasive fungal infections, Methods Mol. Biol. 1508 (2017) 17-65.

[5] J.R. Perfect, The antifungal pipeline: a reality check, Nat Rev Drug Discov. 16 (2017) 603-616.

[6] M.L. Villasmil, A.D. Barbosa, J.L. Cunningham, S. Siniossoglou, J.T. Nickels, An Erg11 lanosterol 14-α-demethylase-Arv1 complex is required for Candida albicans virulence, PLoS ONE. 15 (2020) e0235746.

[7] D.P. Kontoyiannis, R.E. Lewis, Antifungal drug resistance of pathogenic fungi, Lancet. 359 (2002) 1135-1144.

[8] R.S. Shapiro, N. Robbins, L.E. Cowen, Regulatory circuitry governing fungal development, drug resistance, and disease, Microbiol. Mol. Biol. Rev. 75 (2011) 213-267.

[9] B. Sun, Y. Dong, K. Lei, J. Wang, L. Zhao, M. Liu, Design, synthesis and biological evaluation of amide-pyridine derivatives as novel dual-target (SE, CYP51) antifungal inhibitors, Bioorg. Med. Chem. 27 (2019) 2427-2437.

[10] C.M. Calvet, D.F. Vieira, J.Y. Choi, D. Kellar, M.D. Cameron, J.L. Siqueira- Neto, J. Gut, J.B. Johnston, L. Lin, S. Khan, J.H. McKerrow, W.R. Roush, L.M. Podust, 4-Aminopyridyl-Based Cyp51 Inhibitors as Anti-Trypanosoma Cruzi Drug Leads with

Improved Pharmacokinetic Profile and *in Vivo* Potency, J. Med. Chem. 57 (2014) 6989-7005.
[11] M.M. Canuto, F.G. Rodero, Antifungal drug resistance to a zoles and polyenes, Lancet Infect. Dis. 2 (2002) 550-563.
[12] G.I. Lepesheva, L. Friggeri, M.R. Waterman, CYP51 as drug targets for fungi and protozoan parasites: past, present and future, Parasitology.145 (2018) 1820-1836.
[13] Y. Mahmoudi, H. Badali, S.M. Hashemi, M. Ansari, H. Fakhim, M. Fallah, M. Shokrzadeh, S. Emami, New potent antifungal triazole alcohols containing N-benzylpiperazine carbodithioate moiety: Synthesis, in vitro evaluation and in silico study, Bioorg Chem. 90 (2019) 103060.
[14] K.B. Steinbuch, R.I. Benhamou, L. Levin, R. Stein, M. Fridman, Increased Degree of Unsaturation in the Lipid of Antifungal Cationic Amphiphiles Facilitates Selective Fungal Cell Disruption, ACS Infect Dis. 4 (2018) 825-836.
[15] N.T. Chandrika, E.K. Dennis, S.K. Shrestha, H.X Ngo, K.D. Green, S. Kwiatkowski, A.G. Deaciuc, L.P. Dwoskin, D.S. Watt, S. Garneau-Tsodikova, N,N'-diaryl-bishydrazones in a biphenyl platform: Broad spectrum antifungal agents, Eur J Med Chem. 164 (2019) 273-281.
[16] M.K. Kathiravan, A.B. Salake, A.S. Chothe, P.B. Dudhe, R.P. Watode, M.S. Mukta, S. Gadhwe, The biology and chemistry of antifungal agents: a review, Bioorg. Med. Chem. 20 (2012) 5678-5698.
[17] B. Sun, W. Huang, M. Liu, K. Lei, Comparison and analysis of the structures and binding modes of antifungal SE and CYP51 inhibitors, J. Mol. Graph. Model. 77 (2017) 1-8.
[18] C. Sheng, W. Zhang, New lead structures in antifungal drug discovery, Curr. Med. Chem. 18 (2011) 733-766.
[19] Z. Jiang, Y. Wang, W. Wang, S. Wang, B. Xu, G. Fan, G. Dong, Y. Liu, J. Yao, Z. Miao, W. Zhang, C. Sheng, Discovery of highly potent triazole antifungal derivatives by heterocycle-benzene bioisosteric replacement, Eur. J. Med. Chem. 64 (2013) 16-22.
[20] R.I. Benhamou, M. Bibi, K.B. Steinbuch, H. Engel, M. Levin, Y. Roichman, J. Berman, M. Fridman, Real-time imaging of the azole class of antifungal drugs in live Candida cells, ACS Chem. Biol. 12 (2017) 1769-1777.
[21] M. Nowosielski, M. Hoffmann, L.S. Wyrwicz, P. Stepniak, D.M. Plewczynski, M. Lazniewski, K. Ginalski, L. Rychlewski, Detailed Mechanism of Squalene Epoxidase Inhibition by Terbinafine, J. Chem. Inf. Model. 51 (2011) 455-462.
[22] Pooja, P. Prasher, P. Singh, K. Pawar, K.S. Vikramdeo, N. Mondal, S.S. Komath, Synthesis of amino acid appended indoles: appreciable anti-fungal activity and inhibition of ergosterol biosynthesis as their probable mode of action, Eur. J. Med. Chem. 80 (2014) 325-339.
[23] V. Moudgal, J. Sobel, Antifungals to treat Candida albicans, Expert. Opin. Pharmacother. 11 (2010) 2037-2048.

[24] D.A. Enoch, H.A. Ludlam, N.M. Brown, Invasive fungal infections: a review of epidemiology and management options, J. Med. Microbiol. 55 (2006) 809-818.
[25] M.C. Fisher, N.J. Hawkins, D. Sanglard, S.J. Gurr, Worldwide emergence of resistance to antifungal drugs challenges human health and food security, Sci. 360 (2018) 739-742.
[26] M.V. Papadopoulou, G.I. Bloomer, H.S. Lepesheva, M. Rosenzweig, M. Kaiser, B. Aguilera-Venegas, S.R. Wilkinson, E. Chatelain, J.R. Ioset, Novel 3- nitrotriazole-based amides and carbinols as bifunctional antichagasic agents, J. Med. Chem. 58 (2015) 1307-1319.
[27] T.M. Gonzalez Santiago, B. Pritt, L.E. Gibson, N.I. Comfere, Diagnosis of deep cutaneous fungal infections: Correlation between skin tissue culture and histopathology, J. Am. Acad. Dermatol. 71 (2014) 293-301.
[28] M.C. Arendrup, T.F. Patterson, Multidrug-resistant candida: epidemiology, molecular mechanisms, and treatment, J. Infect. Dis. 216 (2017) S445-S451.
[29] Z. Chang, V. Yadav, S.C. Lee, J. Heitman, Epigenetic mechanisms of drug resistance in fungi, Fungal Genet. Biol. 132 (2019) 103253.
[30] Y. Dong, M. Liu, J. Wang, Z. Ding, B.Sun, Construction of antifungal dual- target (SE, CYP51) pharmacophore models and the discovery of novel antifungal inhibitors, RSC Adv. 9 (2019) 26302-26314.
[31] C.W. Murray, M.L. Verdonk, D.C. Rees, Experiences in fragment-based drug discovery, Trends Pharmacol. Sci. 33 (2012) 224-232.
[32] T.Y. Hargrove, L. Friggeri, Z. Wawrzak, A. Qi, W.J. Hoekstra, R.J. Schotzinger, J.D. York, F. Peter Guengerich, G.I. Lepesheva, Structural analyses of Candida albicans sterol 14a-demethylase complexed with azole drugs address the molecular basis of azole-mediated inhibition of fungal sterol biosynthesis, J. Biol. Chem. 292 (2017) 6728-6743.
[33] Y.F. An, Y. Dong, M. Liu, L.Y. Zhao, D.M. Zhao, J. Han, B. Sun, Construction and evaluation of molecular models: Guide and design of novel SE inhibitors, ACS Med. Chem. Lett. 11 (2020) 1152-1159.
[34] I.D. Kuntz, Structure-based strategies for drug design and discovery, Sci. 257 (1992) 1078-1082.
[35] D. Zhao, S. Zhao, L. Zhao, X. Zhang, P. Wei, C. Liu, C. Hao, B. Sun, X. Su, M. Cheng, Discovery of biphenyl imidazole derivatives as potent antifungal agents: design, synthesis, and structure-activity relationship studies, Bioorg. Med. Chem. 25 (2017) 750-758.
[36] B. Sun, Y. Dong , Y.F. An, M. Liu, J. Han , L.Y. Zhao , X.Y. Liu, Design, synthesis and bioactivity evaluation of novel arylalkene-amide derivatives as dual-target antifungal inhibitors, Eur. J. Med. Chem. 205 (2020) 112645
[37] S. Zhao, L. Zhao, X. Zhang, C. Liu, C. Hao, H. Xie, B. Sun, D. Zhao, M. Cheng, Design, synthesis, and structure-activity relationship studies of benzothiazole derivatives as antifungal agents, Eur. J. Med. Chem. 123 (2016) 514-522.

[38] L.Y. Zhao, L.F. Tian, N.N. Sun, Y. Sun, Y.X. Chen, X.R. Wang, S.Z. Zhao, X. Su, D.M. Zhao, M.S. Cheng, Design, synthesis, and structure-activity relationship studies of l-amino alcohol derivatives as broad-spectrum antifungal agents, Eur. J. Med. Chem. 177 (2019) 374-385.
[39] B. Sun, H. Zhang, M. Liu, Z. Hou, X. Liu, Structure-based virtual screening and ADME/T-based prediction analysis for the discovery of novel antifungal CYP51 inhibitors, Medchemcomm. 9 (2018) 1178-1187
[40] J. Nalawade, A. Shinde, A. Chavan, S. Patil, M. Suryavanshi, M. Modak, P. Choudhari, V.D. Bobade, P.C. Mhaske, Synthesis of new thiazolyl-pyrazolyl-1,2,3-triazole derivatives as potential antimicrobial agents, Eur. J. Med. Chem. 179 (2019) 649-659.
[41] S.Z. Zhao, X.Q. Zhang, P. Wei, X. Su, L.Y. Zhao, M.Y. Wu, C.Z. Hao, C.C. Liu, D.M. Zhao, M.S. Cheng, Design, synthesis and evaluation of aromatic heterocyclic derivatives as potent antifungal agents, Eur. J. Med. Chem. 137 (2017) 96-107.
[42] Y. Dong, X.Y. Liu, Y.F. An, M. Liu, J. Han, B. Sun, Potent arylamide derivatives as dual-target antifungal agents: Design, synthesis, biological evaluation, and molecular docking studies, Bioorg. Chem. 99 (2020) 103749.
[43] B. Sun, H. Zhang, Y. Dong, L. Zhao, M. Liu, Evaluation of the combination mode and features of p38 MAPK inhibitors: construction of different pharmacophore models and molecular docking, Mol. Simulat. 45 (2019) 975-984.
[44] G.Y. Han, N. Liu, C.L. Li, J. Tu, Z. Li, C.Q. Sheng, Discovery of Novel Fungal Lanosterol 14α-Demethylase (CYP51)/Histone Deacetylase Dual Inhibitors to Treat Azole-Resistant Candidiasis, J. Med. Chem. 63 (2020) 5341-5359.
[45] P.S. Khakar, Two-dimensional (2D) in silico models for absorption, distribution, metabolism, excretion and toxicity (ADME/T) in drug discovery, Curr. Top. Med. Chem. 10 (2010) 116-126.

Table 1. The scoring values for preferred docking fragments

Name	Fragment structure	Potential Energy	Ludi_Score	
			SE	CYP51
1. 1-naphthoic acid	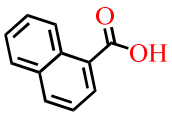	104.9261	331	348
2. 5-Amino-1-benzofuran	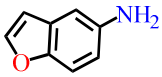	98.9786	279	316
3. Aminomethyl pyridine	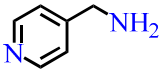	83.0628	308	324
4. 9*H*-pyrido[3,4-*b*] indole	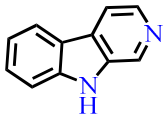	49.2029	287	301
5. 1-ethyl-1H-imidazole	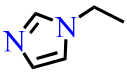	97.1579	301	298
6. N-methyl-1H-imidazole-1 -carboxamide	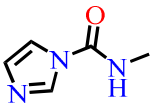	72.7368	284	296
7. 2-Aminoacetophenone	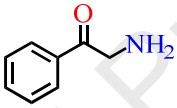	103.2519	314	291
8. N-phenylmethanetriamine	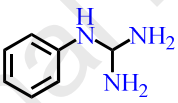	49.0356	252	280
9. Cyclohexaneamine	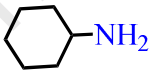	55.6181	279	264
10. Resorcinol	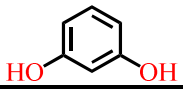	86.6885	249	237

Table 2. *In vitro* antifungal activities of the target compounds (MIC, μg/mL).

Compd	R	MIC, μg/mL				
		C.alb.	***C.gla.***	***C.kru.***	***C.tro.***	***A.fum.***
7a-1	4-aminopyridine	0.5	0.5	0.5	1	8
7a-2	3-aminopyridine	0.25	0.25	0.5	0.25	>16
7a-3	4-pyridinemethaneamine	1	1	2	0.5	8
7a-4	3-pyridinylmethylamine	0.5	2	0.5	0.25	>16
7b-1	4-aminopyridine	0.25	0.5	1	0.25	8
7b-2	3-aminopyridine	0.125	0.25	0.25	0.125	4
7b-3	4-pyridinemethaneamine	0.25	2	0.5	1	8
7b-4	3-pyridinylmethylamine	0.5	0.5	0.25	0.25	>16
10a-1	cyclohexanamine	0.5	0.25	0.5	1	>16
10a-2	cyclopentanamine	0.5	2	0.5	0.5	>16
10a-3	phenylmethanamine	0.5	0.5	1	0.25	8
10a-4	4-methylaniline	0.25	0.25	0.5	0.5	>16
10a-5	4-pyridinemethaneamine	0.25	0.5	0.5	0.25	8
10b-1	cyclohexanamine	0.5	0.25	0.5	0.5	>16
10b-2	cyclopentanamine	0.25	0.25	1	0.5	8
10b-3	phenylmethanamine	0.5	1	1	0.5	>16
10b-4	4-methylaniline	0.125	0.25	0.25	0.25	8
10b-5	4-pyridinemethaneamine	0.25	0.125	0.25	0.25	4
17a-1	H	0.25	0.25	0.5	0.125	8
17a-2	methyl	0.125	0.25	0.25	0.125	4
17a-3	Isopropyl	0. 25	0.5	1	0.5	>16
17b-1	H	0.25	1	0.5	0.25	>16
17b-2	methyl	0.25	0.5	0.25	0.125	8
17b-3	Isopropyl	0.5	1	1	0.5	>16
18a	H	0.5	0.25	0.5	0.25	8
18b	H	0.125	0.25	0.25	0.25	8
Fluconazole	-	0.25	0.25	1	0.25	>16
Naftifine	-	0.5	0.25	2	0.5	8

Abbreviations: ***C. alb.***, *Candida albicans* (ATCC 10231); ***C. gla.***, *Candida glabrata* (ATCC 0001); ***C. kru.***, *Candida krusei* (ATCC 6258); ***C. tro.***, *Candida tropicalis* (ATCC 1369); ***A. fum.***, *Aspergillus fumigatus* (KM8001).

Table 3. *In vitro* antifungal activities of the target compounds (MIC, μg/mL).

Compd	MIC, μg/mL				
	Strain 17#	Strain CaR	Strain 632	Strain 901	Strain 904
7b-2	8	4	>16	>16	>16
10b-5	4	8	8	4	>16
17a-2	2	4	8	4	4
Naftifine	8	>16	8	>16	8
Fluconazole	>16	>16	>16	>16	>16

Abbreviations: strain 17#, **CaR**, **632, 901**, **904,** fluconazole-resistant strain of *Candida albicans*; **Strains 17#** and CaR were provided by Institute of Microbiology, Chinese Academy of Sciences. Strains 632, 901 and 904 were provided by the Second Military Medical University.

Table 4. Analysis of sterol composition in *C.alb.* by LC-MS.[a]

Compd.	Concentration (μg/mL)	% of total sterols (*C. alb.*)				
		Ergosterol	**Squalene**	**Lanosterol**	**Eburicol**	**Unknown sterol**
10b-5[b]	0.125	68.4	9.2	3.8	13.6	5.0
	0.5	35.6	14.5	7.2	37.9	4.8
	4	13.2	20.5	10.9	49.3	6.1
17a-2	0.125	66.4	7.9	2.8	17.5	5.4
	0.5	29.9	21.6	8.7	34.0	5.8
	4	10.8	27.9	12.5	42.6	6.2
Naftifine[c]	0.125	73.5	16.8	3.7	1.9	4.1
	0.5	40.8	39.2	9.4	5.7	4.9
	4	15.9	56.8	12.5	9.7	5.1
Fluconazole	0.125	78.5	-	5.1	12.8	3.6
	0.5	43.9	-	8.9	42.5	4.7
	4	12.7	1.3	16.3	64.5	5.2
Control[d]	-	95.1	-	-	1.4	3.5

[a] Abbreviations: *C.alb.*, *Candida albicans* (ATCC SC5314).

[b] Treated with target compounds **10b-5, 17a-2**.

[c] Treated with naftifine.

[d] Control (no drug).

Table 5. The dual-target (SE, CYP51) enzymatic activity of compounds 10b-5 and 17a-2

Compd	IC_{50} (μM)	
	SE	CYP51
10b-5	0.685	1.253
17a-2	0.961	0.537
Naftifine	0.284	-
Fluconazole	-	0.116

[a] Used as positive control.

Table 6. In vitro human plasma stability of compounds 10b-5 and 17a-2.

Compd	Stability in Human Blood Plasma	
	% Remaining at 60 min	% Remaining at 120 min
10b-5	94.5	91.6
17a-2	96.3	92.1

Table 7. The analysis of plasma biochemical levels with different treatment groups

Group	**AST(IU/L)**	**ALT(IU/L)**	**BUN (mmol/L)**
Saline	104.7±5.2	105±8.3	6.8±0.4
Compound 10b-5	108.6±6.3	102±12.6	7.3±0.9
Compound 17a-2	112.3±5.9	106±7.4	6.4±0.7

Table 8. Molecular docking results of target compound **17a-2** with dual-target (SE, CYP51)

Compd	-CDOCKER ENERGY	-CDOCKER INTERACTION ENERGY	Absolute Energy	Target Enzyme
17a-2	24.53	42.85	57.44	SE
17a-2	21.15	39.92	49.51	CYP51
Naftifine	34.65	47.72	60.67	SE
Fluconazole	27.72	44.76	65.94	CYP51

Table 9. The ADME/T prediction of target compounds compared with the naftifine and fluconazole.

ADME/T parameters	Series 1 compounds	Series 2 compounds	Series 3 compounds	Naftifine	Fluconazole
A log *P*98 [a]	1.638~1.645	2.139~2.741	2.139~3.466	4.863	0.750
PSA[b]	62.025	76.831	84.674, 94.132	3.352	76.556
Aqueous solubility	3	2, 3	2, 3	2	4
HIA[d]	0	0	0	1	0
PPB [e]	Highly bound	Highly bound	Highly bound	Highly bound	Highly bound
BBB penetration [f]	3	3	3	0	3
CYP450 2D6 binding [g]	0	0	0	0	1
Hepatotoxicity	Non-Toxic	Non-Toxic	Non-Toxic	Non-Toxic	Toxic
DTP [h]	Toxic, Non-Toxic	Toxic	Toxic	Toxic	Toxic
FDA[i] rodent carcinogenicity	Non-carcinogen	Non-carcinogen	Non-carcinogen	Non-carcinogen	Non-carcinogen
Ames mutagenicity	Non-mutagen	Non-mutagen	Non-mutagen	Non-mutagen	Non-mutagen
Skin sensitization	Non-irritant	Non-Irritant, Irritant	Non-Irritant, Irritant	Irritant	Irritant
Skin irritating	Non-irritant	Non-irritant	Non-irritant	Mild-irritant	Non-irritant

a. A log P98 (atom-based log *P*) (□-2.0 or □7.0: very low absorption). **b.** PSA (polar surface area) (>150: very low absorption). **c.** Level of aqueous solubility predicted: 0 (extremely low), 1 (very low, but possible), 2 (low), 3 (good), 4 (optimal), 5 (too soluble), 6 (warning: molecules with one or more unknown A log *P* calculations). **d.** HIA (human intestinal absorption), level of human intestinal absorption prediction: 0 (good), 1 (moderate), 2 (poor), 3 (very poor). **e.** PPB, plasma protein binding. **f.** BBB (blood brain barrier), level blood brain barrier penetration prediction: 0 (very high penetrate), 1 (high), 2 (medium), 3 (low), 4 (undefined). **g.** Prediction cytochrome P4502D6 enzyme inhibition (0: non-inhibitor; 1: inhibitor). **h.** DTP, development toxicity potential. **i.** FDA, food and drug administration.

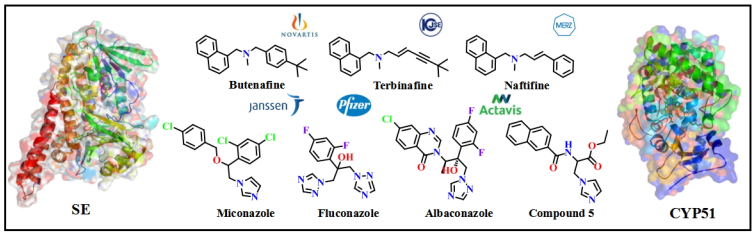

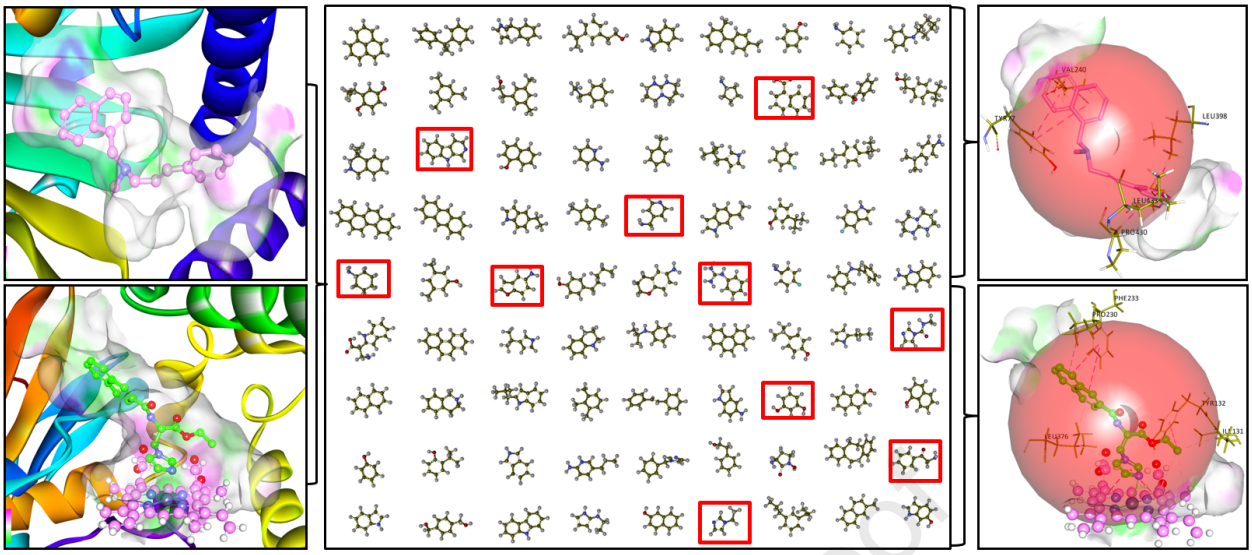

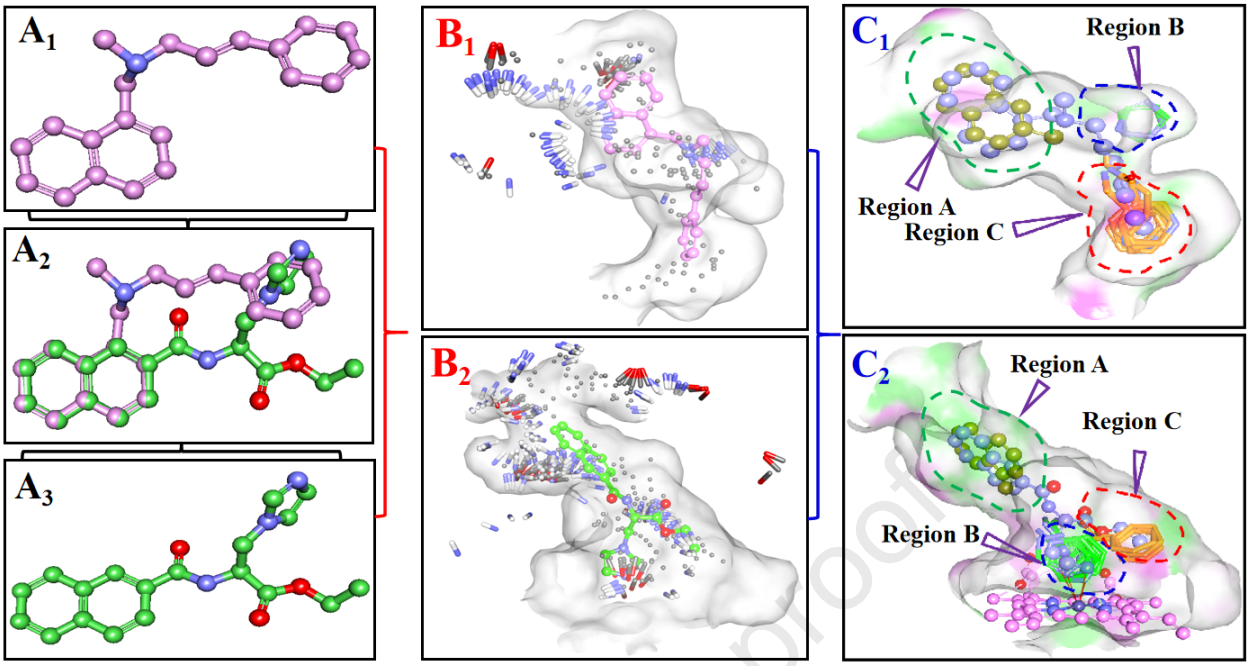

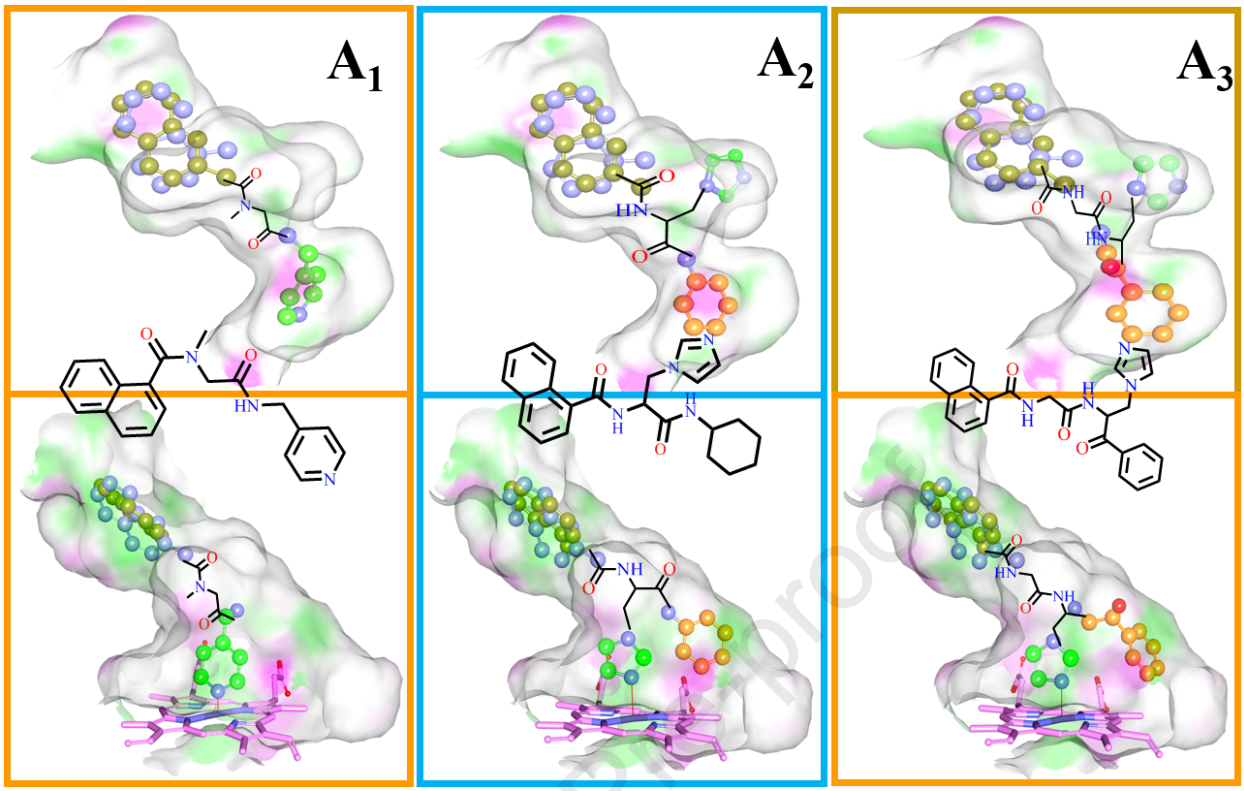

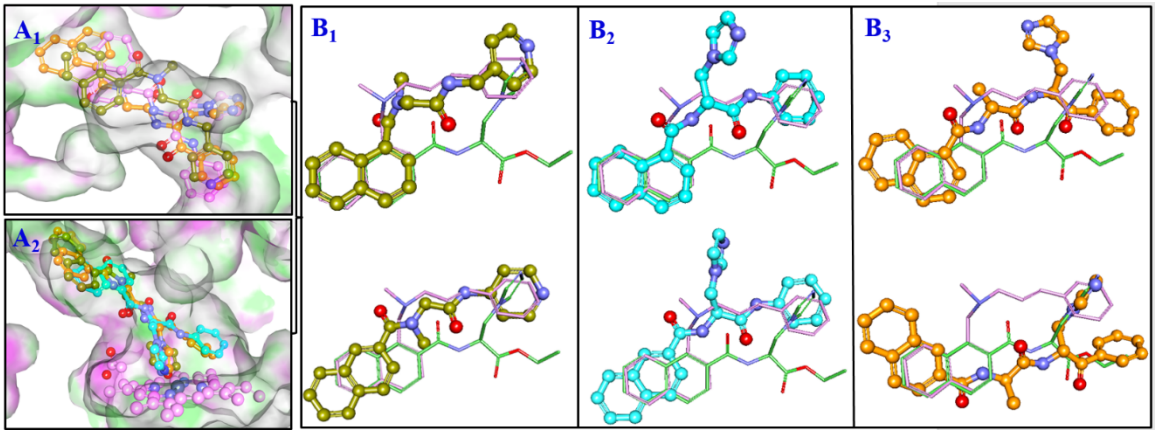

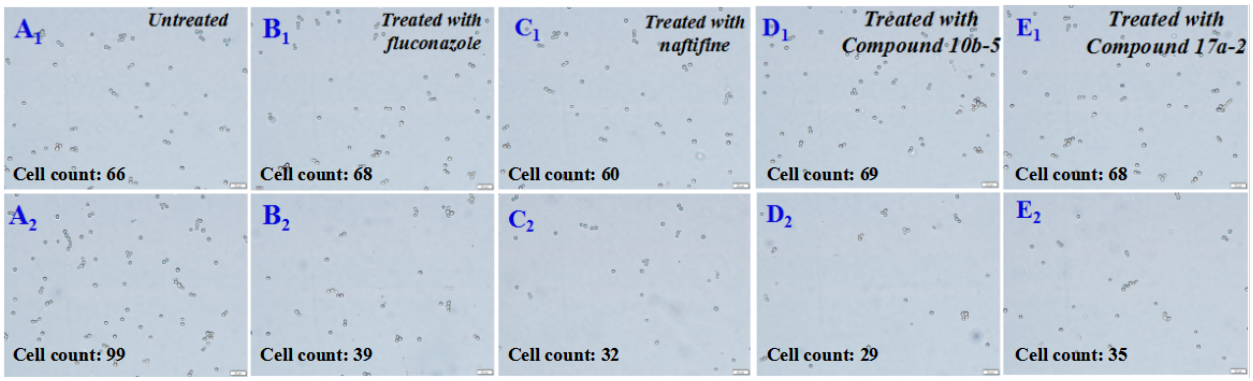

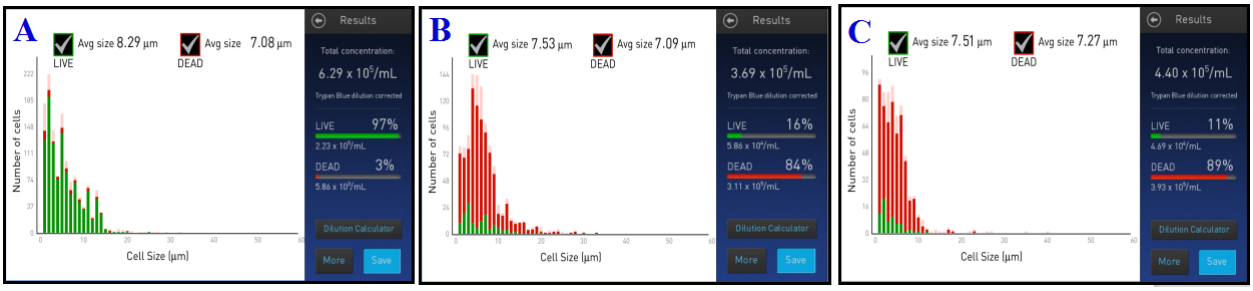

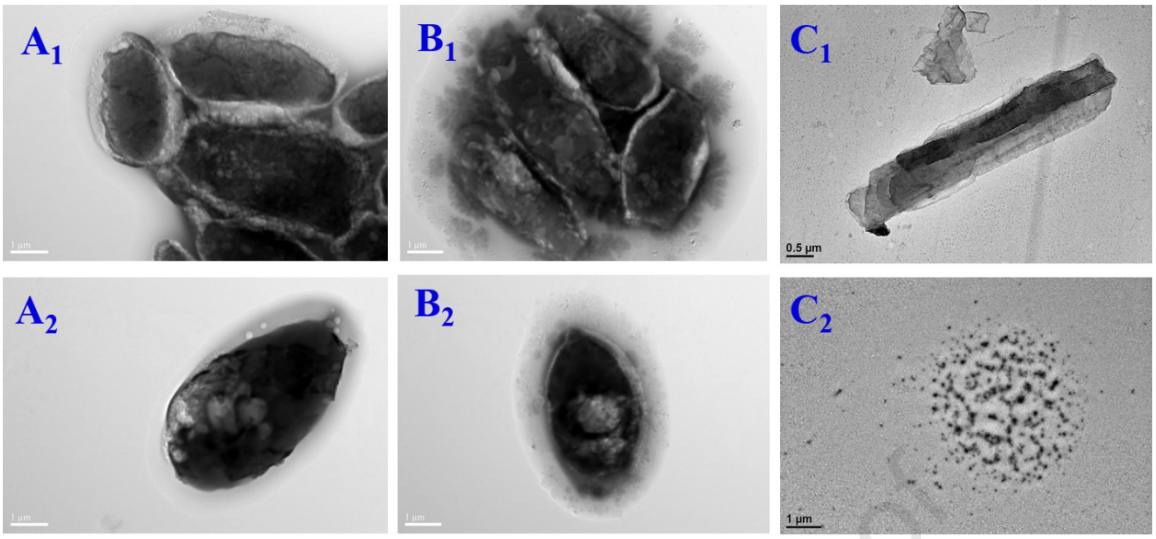

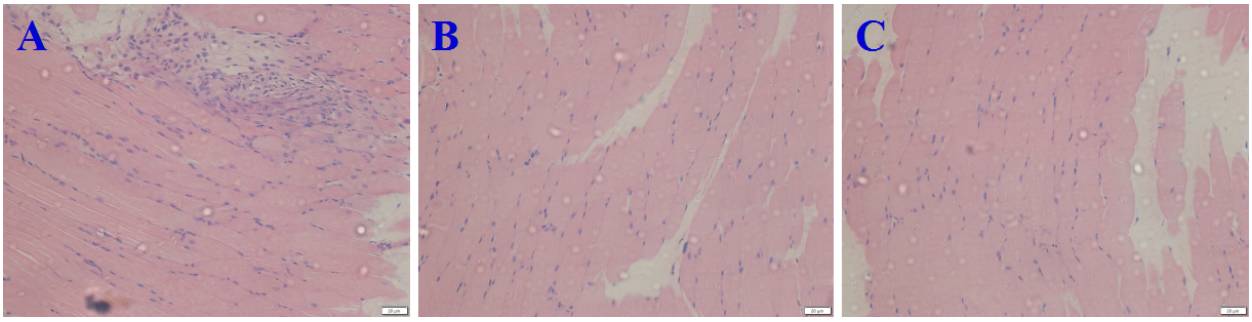

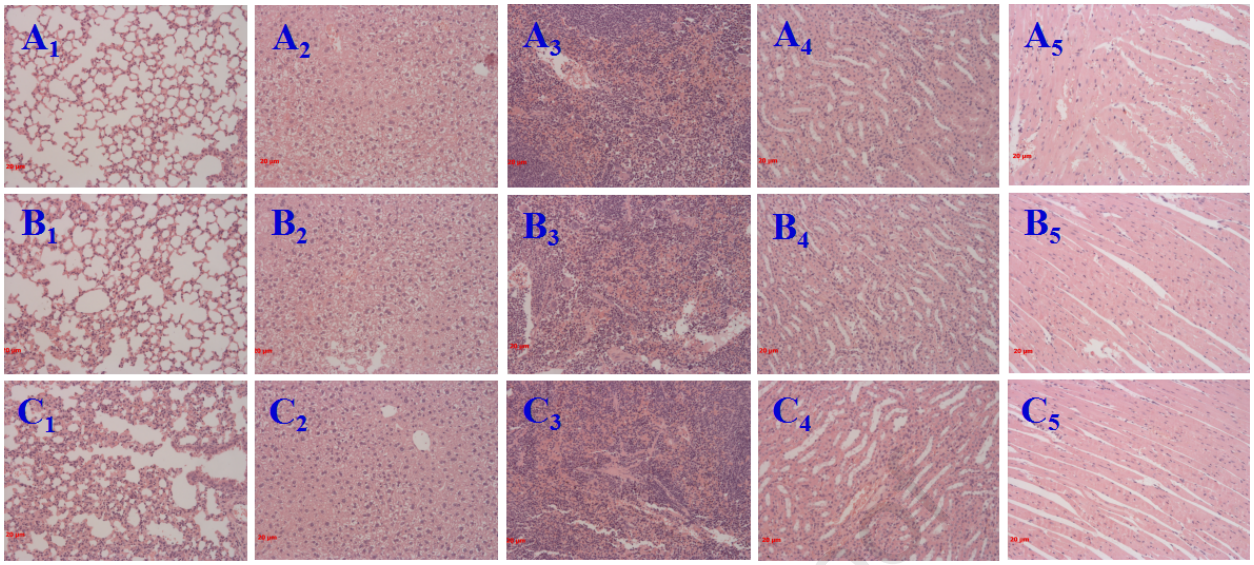

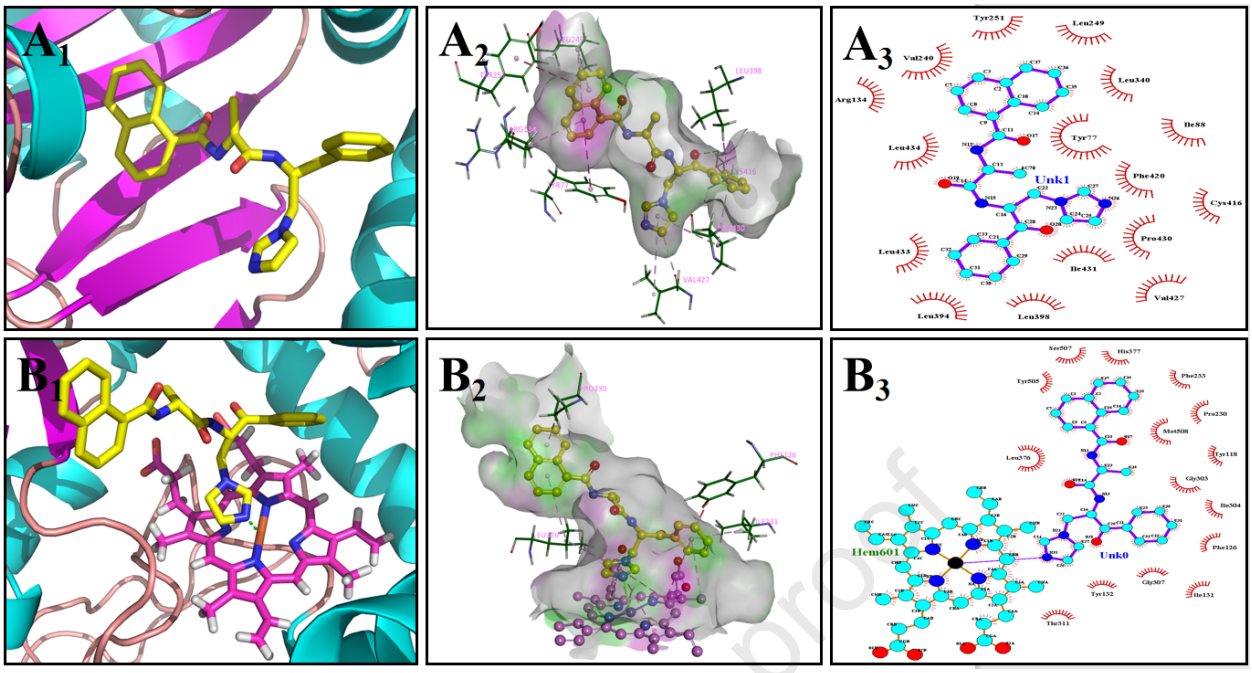

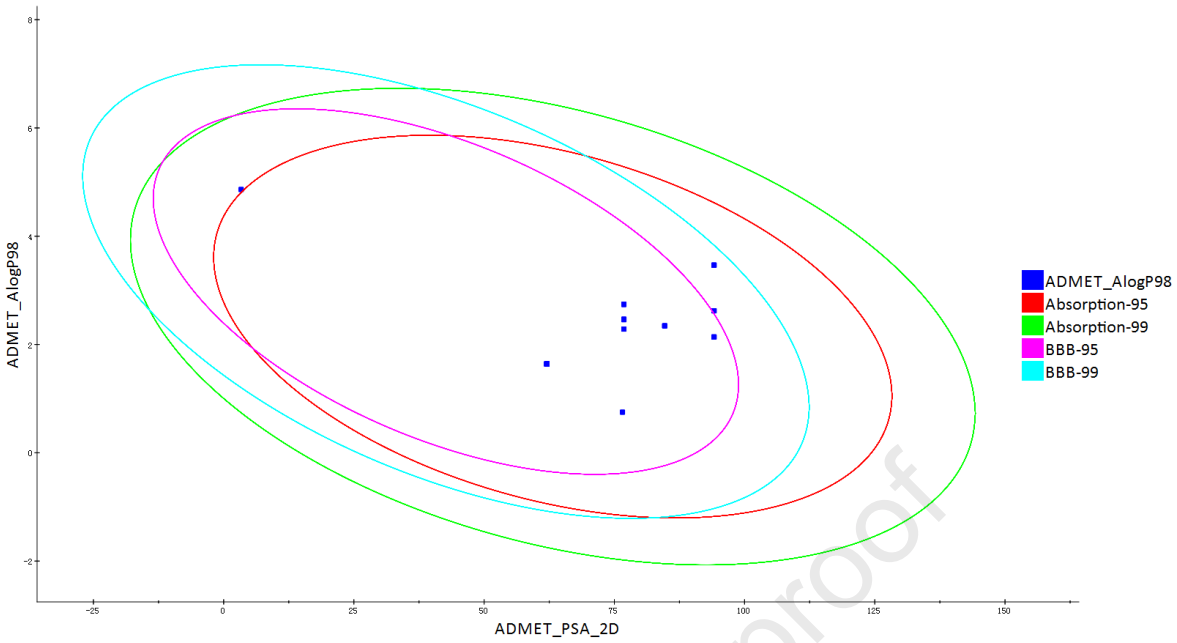

Highlights

1. The novel dual-target antifungal drugs were constructed by fragment-based drug design.

2. Compounds **10b-5** and **17a-2** showed excellent antifungal activity in *vivo* and in *vitro*.

3. Compounds **17a-2** exhibits excellent inhibitory activity against drug-resistant pathogenic fungi.

4. Preliminary mechanism studies of compound **10b-5** and **17a-2** were proved.

5. The target compounds **10b-5** and **17a-2** show excellent drug-forming properties.

Declaration of Interest Statement

The authors declare that they have no known competing financial interests or personal relationships that could have appeared to influence the work reported in this paper.